# Lattice model of equilibrium polymerization. VII. Understanding the role of "cooperativity" in self-assembly

**ARTICLE** *in* THE JOURNAL OF CHEMICAL PHYSICS · JUNE 2008

Impact Factor: 2.95 · DOI: 10.1063/1.2909195 · Source: PubMed

# Lattice model of equilibrium polymerization. VII. Understanding the role of "cooperativity" in self-assembly

Jack F. Douglas,[1,a)] Jacek Dudowicz,[2,b)] and Karl F. Freed[2,c)]
[1]*Polymers Division, National Institute of Standards and Technology, Gaithersburg, Maryland 20899, USA*
[2]*The James Franck Institute and the Department of Chemistry, The University of Chicago, Chicago, Illinois 60637, USA*

(Received 29 February 2008; accepted 21 March 2008; published online 9 June 2008)

Cooperativity is an emergent many-body phenomenon related to the degree to which elementary entities (particles, molecules, organisms) collectively interact to form larger scale structures. From the standpoint of a formal mean field description of chemical reactions, the cooperativity index $m$, describing the number of elements involved in this structural self-organization, is the order of the reaction. Thus, $m$ for molecular self-assembly is the number of molecules in the final organized structure, e.g., spherical micelles. Although cooperativity is crucial for regulating the thermodynamics and dynamics of self-assembly, there is a limited understanding of this aspect of self-assembly. We analyze the cooperativity by calculating essential thermodynamic properties of the classical $m$th order reaction model of self-assembly ($\mathcal{FA}m$ model), including universal scaling functions describing the temperature and concentration dependence of the order parameter and average cluster size. The competition between self-assembly and phase separation is also described. We demonstrate that a sequential model of thermally activated equilibrium polymerization can quantitatively be related to the $\mathcal{FA}m$ model. Our analysis indicates that the essential requirement for "cooperative" self-assembly is the introduction of constraints (often nonlocal) acting on the individual assembly events to regulate the thermodynamic free energy landscape and, thus, the thermodynamic sharpness of the assembly transition. An effective value of $m$ is defined for general self-assembly transitions, and we find a general tendency for self-assembly to become a true phase transition as $m \to \infty$. Finally, various quantitative measures of self-assembly cooperativity are discussed in order to identify experimental signatures of cooperativity in self-assembling systems and to provide a reliable metric for the degree of transition cooperativity. © *2008 American Institute of Physics*. [DOI: 10.1063/1.2909195]

## I. INTRODUCTION

Debye pioneered the modeling of the self-assembly of compact structures, such as micelles,[1,2] and his model continues to be applied for determining the free energy parameters governing micelle formation.[3–5] The underlying theory is also used to treat a wide spectrum of self-assembly phenomena, ranging from DNA hybridization,[6,7] to the formation of metal oxide clusters[8] and numerous biological structures, including the capsid shells of viruses.[9–11]

The Debye model[1] of micelle formation is sometimes called the "closed association model" because it idealizes the self-assembly of micelles as formally a reversible $m$th order chemical reaction in which $m$ identical (e.g., surfactant) species $M$ *directly associate* into a fully assembled entity $M_m$,

$$mM \rightleftharpoons M_m. \tag{1}$$

Below this model is called the $m$th order free association model or the $\mathcal{FA}m$ model. The type of organization in Eq. (1) evidently requires the existence of highly "cooperative" intermolecular interactions, and the parameter $m$ is often taken as a measure of the "cooperativity" of self-assembly. In the biological literature, as exemplified by a recent paper on DNA hybridization,[6,7] the parameter $m$ has also been termed the "molecularity" of self-assembly.[6,7] As discussed below, the "cooperativity index" $m$ is important in influencing the sharpness of the self-assembly transition. Moreover, cooperativity provides a switching mechanism for many biological processes that are essential to living systems,[12–16] and cooperativity can profoundly affect the kinetics of self-assembly (see Discussion).

At the other extreme, the chainlike growth of wormlike micelles[17] and other supramolecular assemblies under equilibrium conditions has traditionally been analyzed with a class of self-assembly models that are perfectly *uncooperative* (termed "isodesmic" self-assembly[18]). Growth processes in these uncooperative systems are assumed to occur through a cascade of independent steps where molecules (or particles or micelle segments) add or depart sequentially and independently from the assemblage to form the growing chain structures. Each step in this process involves an association at equilibrium, and the average chain length arises from a balance of the rates for chain formation and disintegration and is thus governed by temperature, the concentration of the associating species, and other thermodynamic

a)Electronic mail: dudowicz@jfi.uchicago.edu.
b)Electronic mail: jack.douglas@nist.gov.
c)Electronic mail: freed@uchicago.edu.

 

variables that influence the interparticle interactions. Importantly, the structures can grow unbounded in size as the temperature approaches zero for uncooperative systems, and there is no kinetic lag as observed for cooperative self-assembly processes.[18] This uncooperative model of self-assembly is designated here as the "free association" ($\mathcal{FA}$) model.[19] Because of its relative simplicity, the $\mathcal{FA}$ model has been applied to describe numerous self-assembly processes in which growth of the self-assembled structures is unlimited (e.g., formation of wormlike micelles[17]). For example, an off-lattice version of the $\mathcal{FA}$ model has recently been considered by Sciortino *et al.*[20] to treat equilibrium polymerization of linear chains and by Van Workum and Douglas[21] to study the Stockmayer fluid, a system in which dipolar particles reversibly assemble into chains upon cooling. The $\mathcal{FA}$ model has also been used to describe a diverse spectrum of biologically important self-assembling systems, such as the *in vitro* assembly of FTsZ proteins (a bacterial homolog of tubulin[18,22]) into polymeric structures (that are essential to bacterial cell division[23]), the formation of chain-like assemblies of lactoglobulin,[24] the assembly of (guanosine diphosphate) GDP-tubulin,[18,22] etc. Other applications of this model include treatments of hydrogen bonding[25–27] and dipolar fluids,[28] and even supermolecular chain assemblies, such as metal-complex gelator systems.[29–31]

The perfect lack of cooperativity in the $\mathcal{FA}$ model leads to striking differences in behavior from cooperative assembly processes such as micelle formation. For example, the assembly transition becomes so broad in the $\mathcal{FA}$ system that there is no discernable "critical concentration" for the self-assembly process,[18] as normally found in the formation of spherical micelles. Nevertheless, the growth of long chains of unbounded length by equilibrium association greatly affects the critical properties of the free association fluids when they phase separate.[32] Romberg *et al.*[18] summarized physical aspects of uncooperative and cooperative self-assembly, and we discuss these features from a mathematical standpoint below.

The idealized cooperative and uncooperative self-assembly models have been supplemented by more physically realistic "hybrid" models that have been developed to describe the formation of spherical micelles[33–35] and a variety of biological structures. For instance, the popular Kegeles model[33–35] incorporates an initial "nucleation" or "activation" step into the chain of association-dissociation equilibria of the self-assembly process, along with a cutoff $m$ on the ultimate assembly size. These models introduce the equilibrium constant for activation as the product of a "cooperativity factor" $f$ and the equilibrium constant for chain propagation. Thus, the added constraints on the chain of association steps somehow impart cooperativity into the assembly process. Recent dynamic light scattering, microcalorimetry, and cryogenic electron microscopy measurements,[36–39] as well as molecular dynamics simulations,[40] all confirm that sequential models with additional constraints are physically more appropriate for describing the self-assembly of micelles than are the individual $\mathcal{FA}m$ and $\mathcal{FA}$ models of assembly.

The phenomenological success, widespread use, and simplicity of the "closed association" $\mathcal{FA}m$ model and its more recent generalizations motivate our interest in examining the physical origin of the parameter $m$. Normally, this parameter is just "specified" or fit to experimental data using the $\mathcal{FA}m$ model, but we seek instead to elucidate the underlying mechanistic basis of this parameter. The process of DNA hybridation[6,7] and the growth of multistranded fibers[41] are phenomena where $m$ is evidently related to the number of chains in the self-assembling fiber structures, but in other systems, $m$ is an *emergent property* that arises due to complex many-body interactions. More specifically, our investigation is driven by the following questions.

(a) What does it really mean for molecules or particles to cooperatively organize into a structure containing $m$ particles?
(b) What determines the value of $m$? At first glance, the $\mathcal{FA}m$ model seems to be rather artificial since it requires accepting that $m$ molecules, where $m$ is often very large $[m \sim \mathcal{O}(100)]$, *simultaneously* coordinate their motions to assemble directly into some complicated structure having a rather specific geometry. Yet, the thermodynamics of the self-assembly often seems to accord remarkably well with predictions of this simple model and its variants, leading to a very sharp, apparently "all or nothing" transition[6,7] between disordered and ordered states, a phenomenon reminiscent of a true phase transition, such as crystallization.
(c) Does the $\mathcal{FA}m$ system exhibit a true phase transition as $m \to \infty$, and, if so, what kind?

Based on these observations and questions, our analysis begins by considering well studied models of sequential growth/decay equilibrium polymerization for which we have previously shown that the average degree of polymerization naturally saturates to a finite limit $m$ at low temperatures.[32,42] Thus, the effective $m$ naturally emerges from the thermodynamics of a sequential association process, rather than being artificially fixed in advance. More specifically, we find that the magnitude of the cluster size at low temperatures can be defined in terms of more physically transparent properties, such as the concentration of "initiator" molecules (added to the system to begin the cluster growth[42]) or the equilibrium constant for the thermal activation of the associating species that controls the whole polymerization process.[32] Our analysis then focuses on the extent to which this class of exactly solvable models for sequential growth/decay provides insight into the phenomenological parameter $m$ of the $\mathcal{FA}m$ model by comparing and analyzing the properties of all these models.

Section II provides the basic theoretical background of the models that are compared. Section III, in turn, describes our calculations indicating that the simple closed association model can be well represented by the activated association model when $m$ is reasonably large ($m \geqslant 30$). Thus, some basic insights into the physical origins of $m$ are directly elucidated by simple direct comparison of these two models. This correspondence demonstrates that the initial volume fraction $\phi_1^0$ of the association species and the entropies of activation and polymerization ($\Delta s_a$ and $\Delta s_p$) determine the magnitude

of the parameter $m$, which, in turn, dictates the sharpness of the self-assembly transition. Section IV discusses other aspects of cooperativity that emerge from analyzing models of equilibrium polymerization besides the $\mathcal{FA}m$ model.

## II. FLORY–HUGGINS THEORY OF EQUILIBRIUM POLYMERIZATION

The present section summarizes the thermodynamic characteristics of the $\mathcal{FA}m$ model and compares them with those previously analyzed by us[19,32] for the free association ($\mathcal{FA}$) and the activated equilibrium polymerization ($\mathcal{A}$) models. Before polymerization, the constant volume $V$ associating system consists of $n_s$ solvent molecules and $n_1^0$ molecules of the associating species $M$. The system is described by using standard Flory–Huggins (FH) theory for polydisperse polymer solutions. Within this approach, single site occupancy constraints apply to solvent molecules and to all monomers (unreacted monomers and those in aggregates). Consequently, the volume fraction $\phi_1^0=n_1^0/(n_1^0+n_s)$ uniquely determines the composition of the system before polymerization. The constraint of incompressibility (i.e., an infinite pressure) is intrinsic to classic (FH) theory and implies the simplification that the absolute temperature $T$ and the composition $\phi_1^0$ are the only relevant intensive thermodynamical variables. The composition of the system after polymerization is thus a function of $T$, $\phi_1^0$, and the free energy parameters that reflect the strength of the affinity for association.

Although equilibrium polymerization theory was originally derived for the self-assembly of linear polymer chains, the resulting mean field description is insensitive to the topological structure of the assembling species. Consequently, our theory can be considered as a simplified model of self-assembly generally, just as FH theory provides a simplified general treatment of phase separation. Thus, the terms polymerization and self-assembly transitions are interchangeably used below. It should be appreciated, however, that the self-assembly of compact and branched polymer structures involves the formation of multifunctional contacts and the emergence of rigidity effects[43] in the assembled species, and both these factors must be incorporated into the theory to ensure the applicability of equilibrium self-association theory to these other types of self-assembly.

### A. Characterization of the models of equilibrium polymerization

Within the $\mathcal{FA}$ model, each molecule of species $M$ can freely associate into clusters whose growth may proceed either by addition of a single monomer or by the linkage of two aggregates. Since all these processes are assumed to occur in equilibrium, clusters may also break into two smaller aggregates, or segments may dissociate from clusters. The above two modes of polymerization are coveniently expressed by the single kinetic equation,[19]

$$M_j + M_k \rightleftharpoons M_{j+k}, \quad j,k = 1,2,\ldots,\infty. \tag{2}$$

The cluster size distribution is governed by the equilibrium constant $K_p(T)$ for the polymerization reaction in Eq. (2) that is defined in terms of the enthalpy $\Delta h_p$ and entropy $\Delta s_p$ of polymerization in the standard fashion,

$$K_p(T) = \exp[-(\Delta h_p - T\Delta s_p)/(k_B T)], \tag{3}$$

where $k_B$ designates Boltzmann's constant. For simplicity, both $\Delta h_p$ and $\Delta s_p$ are taken as identical for all $j$ and $k$ and as independent of temperature. The independence of $K_p(T)$ on pressure stems from the assumed incompresibility of the system, an assumption that may be lifted to describe constant pressure systems.[44]

The $\mathcal{FA}m$ model is a simplified version of the $\mathcal{FA}$ model and is predicated on the assumption that $m$ monomer molecules simultaneously combine into an $m$-cluster of fixed composition according to the reaction,

$$mM_1 \rightleftharpoons M_m. \tag{4}$$

In contrast to the equilibrium $\mathcal{FA}$ system, the $\mathcal{FA}m$ counterpart is composed only of monomers $M_1$ and monodisperse clusters $M_m$ in addition to the solvent molecules that, as mentioned above, are present but do not participate in the association processes. Cluster-solvent interactions are, however, responsible for the system's phase separation which is affected by the self-assembly. The equilibrium constant $K_{p,m}(T)$,

$$K_{p,m}(T) \equiv \exp[-(\Delta h_{p,m} - T\Delta s_{p,m})/(k_B T)], \tag{5}$$

for the reaction in Eq. (4) may formally be related to the equilibrium constant $K_p(T)$ for the association reaction in Eq. (2) by the simple scaling $K_{p,m}=K_p^{(m-1)}$ which, in turn, establishes relations between the corresponding free energy parameters for these two reactions as $\Delta h_{p,m}=(m-1)\Delta h_p$ and $\Delta s_{p,m}=(m-1)\Delta s_p$.

The activated self-assembly model $\mathcal{A}$ considered here is described by the reaction scheme,[19,45]

$$M_1 \rightleftharpoons M_1^*, \tag{6}$$

$$M_1^* + M_1 \rightleftharpoons M_2, \tag{7}$$

$$M_i + M_1 \rightleftharpoons M_{i+1}, \quad i = 2,3,\ldots,\infty, \tag{8}$$

where the activated species $M_1^*$ reacts only with nonactivated monomers $M_1$ to form dimers, but $M_1^*$ does not participate in the successive chain propagation steps. An alternative model, in which dimers are formed by linking two activated monomers $M_1^*$ and in which chain growth exclusively occurs through the addition of $M_1^*$ to the resulting polymers, is mathematically isomorphic to that given by Eqs. (6)–(8).[19] The *constraint* of thermal activation on the growth process implies the presence of two additional free energy parameters, the enthalpy $\Delta h_a$ and the entropy $\Delta s_a$ of activation that uniquely specify the equilibrium constant $K_a(T)$ for the activation process in Eq. (6),

$$K_a(T) = \exp[-(\Delta h_a - T\Delta s_a)/(k_B T)]. \tag{9}$$

Thermal activation controls the sharpness of the self-assembly transition through the relative magnitudes of $K_a(T)$ and $K_p(T)$.[19,46] The limit $K_a \to 0$ converts the generally rounded $\mathcal{A}$ model assembly transition into a second order

phase transition. When $K_a=1$ (i.e., $\Delta h_a=\Delta s_a=0$), the $\mathcal{A}$ model coincides with the $\mathcal{FA}$ model that predicts a rather broad polymerization transition. (The helix-coil transition and the ordering in magnetic spin systems with applied magnetic field[47] can both be formally represented in terms of the activated equilibrium polymerization model,[48,49] so that our results below have a broad applicability.) The next subsection summarizes expressions for thermodynamic properties of associating solutions that are used in comparing the three association models considered.

### B. Comparison of models of equilibrium polymerization

The basic variable appearing in the FH expressions for the thermodynamic properties of associating solutions is the product of the equilibrium constant $K_p$ and the volume fraction $\phi_1$ of monomers in the equilibrium mixture after clustering. This variable is designated as

$$A \equiv \phi_1 K_p, \tag{10}$$

for all models of equilibrium polymerization.[19] While $A$ is always positive, it must be less than unity for the $\mathcal{FA}$ and $\mathcal{A}$ models, but no such restriction applies for the $\mathcal{FA}m$ model. Within FH theory, the volume fractions $\{\phi_i\}$ of the associates $\{i\}$ are given by the generalized expressions,

$$\phi_m = mCA^m, \quad \text{for a single } m \geqslant 2, \quad \mathcal{FA}m \text{ model}, \tag{11}$$

and

$$\phi_i = iCA^i, \quad i \geqslant 2, \quad \mathcal{FA} \text{ and } \mathcal{A} \text{ models}, \tag{12}$$

where the prefactor $C$ is defined[19] as

$$C = \frac{z}{2\alpha K_p}, \quad \mathcal{FA} \text{ and } \mathcal{FA}m \text{ models}, \tag{13}$$

and

$$C = \frac{zK_a}{2\alpha K_p}, \quad \mathcal{A} \text{ model}, \tag{14}$$

with $z$ being the lattice coordination number (taken as $z=6$) and with the stiffness parameter $\alpha$ ranging from unity for stiff chains to $(z-1)$ for completely flexible chains. The mass conservation condition relates the initial monomer concentration $\phi_1^0$ to $\phi_1$, and the form of the condition varies with the model,

$$\phi_1^0 = \phi_1 + mCA^m, \quad A > 0, \quad \mathcal{FA}m \text{ model}, \tag{15}$$

$$\phi_1^0 = \phi_1 + \frac{CA^2(2-A)}{(1-A)^2}, \quad 0 < A < 1, \quad \mathcal{FA} \text{ model}, \tag{16}$$

$$\phi_1^0 = \phi_1 + \phi_1^* + \frac{CA^2(2-A)}{(1-A)^2}, \quad 0 < A < 1, \quad \mathcal{A} \text{ model}. \tag{17}$$

The average degree $L$ of polymerization ("chain length") is given by

$$L \equiv \frac{\phi_1 + \phi_m}{\phi_1 + (\phi_m/m)} = \frac{\phi_1^0}{\phi_1^0 - CA^m(m-1)}, \quad \mathcal{FA}m \text{ model}, \tag{18}$$

$$L \equiv \frac{\Sigma_{i=1}^{\infty}\phi_i}{\Sigma_{i=1}^{\infty}(\phi_i/i)} = \frac{\phi_1^0}{\phi_1^0 - \dfrac{CA^2}{(1-A)^2}}, \quad \mathcal{FA} \text{ model}, \tag{19}$$

$$L \equiv \frac{\phi_1^* + \Sigma_{i=1}^{\infty}\phi_i}{\phi_1^* + \Sigma_{i=1}^{\infty}(\phi_i/i)} = \frac{\phi_1^0}{\phi_1^0 - \dfrac{CA^2}{(1-A)^2}}, \quad \mathcal{A} \text{ model}. \tag{20}$$

The extent of polymerization $\Phi$ ("order parameter" for self-assembly) is defined as the fraction of monomers converted into polymers and has a closed form expression,

$$\Phi \equiv \frac{\phi_1^0 - \phi_1}{\phi_1^0} = \frac{mCA^m}{\phi_1^0}, \quad \mathcal{FA}m \text{ model}, \tag{21}$$

$$\Phi \equiv \frac{\phi_1^0 - \phi_1}{\phi_1^0} = \frac{1}{\phi_1^0}\frac{CA^2(2-A)}{(1-A)^2}, \quad \mathcal{FA} \text{ and } \mathcal{A} \text{ models}. \tag{22}$$

The specific heat is another important thermodynamic property of equilibrium associating solutions that is readily evaluated from our theory (albeit not always easily accessible experimentally). The constant volume specific heat $C_V$ (exclusive of vibrational contributions) equals,

$$\frac{C_V}{N_l k_B} = \left(\frac{\Delta h_p}{k_B T}\right)^2 \frac{(m-1)^2 CA^m}{1 + m^2 K_p CA^{m-1}}, \quad \mathcal{FA}m \text{ model}, \tag{23}$$

$$\frac{C_V}{N_l k_B} = \left(\frac{\Delta h_p}{k_B T}\right)^2 \frac{CA^2}{(1-A)^3}\left[\frac{2\phi_1^0}{\phi_1^0 + \dfrac{2CA^2}{(1-A)^3}} - (1-A)\right], \quad \mathcal{FA} \text{ model}, \tag{24}$$

$$\frac{C_V}{N_l k_B} = \left(\frac{\Delta h_p}{k_B T} - \frac{\Delta h_a}{k_B T}\right)^2 \frac{CA^2}{(1-A)^3}\left[\frac{2\phi_1^0}{\phi_1^0 + \dfrac{2CA^2}{(1-A)^3}} - (1-A)\right] + \left(\frac{\Delta h_a}{k_B T}\right)^2 \frac{\phi_1}{\phi_1^0 + \dfrac{2CA^2}{(1-A)^3}}\left[\phi_1^0 - \phi_1 + \frac{2CA^2}{(1-A)^3}\right] + 2\left(\frac{\Delta h_p}{k_B T} - \frac{\Delta h_a}{k_B T}\right)\left(\frac{\Delta h_a}{k_B T}\right)\frac{\phi_1}{\phi_1^0 + \dfrac{2CA^2}{(1-A)^3}}\frac{2CA^2}{(1-A)^3}, \quad \mathcal{A} \text{ model}, \tag{25}$$

where $N_l=n_1^0+n_s$ is the sum of the numbers of solvent molecules and monomers of the associating species $M$ (before polymerization) in the system. The system is assumed to be incompressible, and $C_V$ is only approximately equal to the conventionally measured specific heat at constant pressure which is described in Ref. 44.

The self-assembly (polymerization) transition temperature $T_p$ may be determined from the temperature variation of several thermodynamical properties, including the extent of association $\Phi$ or the specific heat $C_V$. Specifically, $T_p$ may be identified with the temperature $T_\Phi$ where the order parameter $\Phi(T)$ exhibits an inflection point or with the temperature $T_{C_V}$ where the specific heat achieves a maximum.[19] While $T_\Phi$ always coincides with $T_{C_V}$ for the activated assembly model, these temperatures (inconveniently) differ for the $\mathcal{FA}$ model.[19] Another definition of $T_p$ is based on the temperature $T_{1/2}$ at which the extent of self-assembly $\Phi(\phi_1^0=\text{const})$ achieves the intermediate value[20] of 1/2. When the self-assembly transition is "rounded," $T_\Phi$, $T_{C_V}$, and $T_{1/2}$ can significantly depart from the *ideal* polymerization temperature $T_p^{(0)}$ predicted by the Dainton–Ivin equation,[19]

$$T_p^{(0)} = \frac{\Delta h_p}{\Delta s_p + k_B \ln \phi_1^0}. \tag{26}$$

Equation (26) is *exact only* when the self-assembly transition becomes a second order transition. Correspondingly, the rearranged form of Eq. (26),

$$T_p = \frac{\Delta h_{\text{vH}}}{\Delta s_{\text{vH}} + k_B \ln \phi_1^0}, \tag{27}$$

is often assumed to describe real associating systems where transition rounding may exist. The free energy parameters of Eq. (27) are called the van't Hoff enthalpy $\Delta h_{\text{vH}}$ and van't Hoff entropy $\Delta s_{\text{vH}}$ of self-assembly and generally depart from the true enthalpy $\Delta h_p$ and entropy $\Delta s_p$ of propagation, respectively (see below). The dependence of $T_p$ on $\phi_1^0$ is termed the *polymerization transition line*, which is the basic thermodynamic observable used for determining $\Delta h_{\text{vH}}$ and $\Delta s_{\text{vH}}$ and which is employed together with the phase boundary to quantify the competition between the self-assembly and phase separation.

While our treatment describes the above thermodynamic properties $(L, \Phi, C_V, T_p)$ as independent of the strength of the isotropic interaction parameter $\chi = \epsilon_{\text{FH}}/T$ (the dimensionless effective interaction energy between the solvent and monomers of the associating species $M$ in an incompressible system), other thermodynamic quantities, such as the spinodal, coexistence curve, second virial coefficient, critical temperature, and critical composition for phase separation, etc., are highly sensitive to the magnitude of $\epsilon_{\text{FH}}$.[19,32,50,51] For instance, the spinodal stability condition for the three association models emerges as,

$$\frac{1}{1-\phi_1^0} + \frac{\phi_1}{\phi_1^2 + m(\phi_1^0 - \phi_1)} - 2\chi = 0, \quad \mathcal{FA}m \text{ model}, \tag{28}$$

$$\frac{1}{1-\phi_1^0} + \frac{1}{\phi_1^0 + \frac{2CA^2}{(1-A)^3}} - 2\chi = 0, \quad \mathcal{FA} \text{ and } \mathcal{A} \text{ models}, \tag{29}$$

where the monomer volume fraction $\phi_1$ (or equivalently $A$) is numerically determined from the corresponding mass conservation condition in Eqs. (15)–(17). Equations (28) and (29) are derived by using the convenient duality of FH equilibrium association theory that enables a multicomponent polydisperse polymer solution to be treated as an effectively binary system.[19]

The free energy parameters for the $\mathcal{FA}m$ model are represented here in terms of the enthalpy $\Delta h_p$ and entropy $\Delta s_p$ for a single propagation step $M_i + M_1 \rightleftharpoons M_{i+1}$ rather than in terms of the enthalpy $\Delta h_{p,m}$ and entropy $\Delta s_{p,m}$ for the formation of an $m$-cluster directly from $m$ monomer molecules [i.e., with Eq. (4)] in order to facilate comparisons between the $\mathcal{FA}$, $\mathcal{A}$, and $\mathcal{FA}m$ (for various $m$) models.

### C. Basic thermodynamic relations for the $\mathcal{FA}m$ model

Several additional themodynamic properties are useful for characterizing the $\mathcal{FA}m$ model, including the equilibrium constant $K_{p,m}^{(\phi)}(T)$ [for the self-assembly reaction in Eq. (4)],

$$K_{p,m}^{(\phi)}(T) \equiv \frac{\phi_m}{\phi_1^m}, \quad m \geqslant 2, \tag{30}$$

which is thereby simply related to the equilibrium constant $K_{p,m}(T)$ of Eq. (5) as

$$K_{p,m}^{(\phi)}(T) = K_{p,m}(T)\left[\frac{mz}{2\alpha}\right], \quad m \geqslant 2. \tag{31}$$

Equation (30) is a definition whose strict interpretation implies ideal system where the activities can be replaced by concentrations. The $K_{p,m}^{(\phi)}$ is more accessible to direct measurements than is $K_{p,m}(T)$ due to the existence of a straightforward relation between $K_{p,m}^{(\phi)}$ and the order parameter $\Phi$ for self-assembly,

$$K_{p,m}^{(\phi)}(T) = \frac{\Phi}{(1-\Phi)^m (\phi_1^0)^{(m-1)}}, \tag{32}$$

an important relation that is consistent with Eq. (5) of Ref. 6. [The absence of an extra factor of $m$ in Eq. (32) arises from our choice of volume fractions as concentration units.] Defining the self-assembly transition temperature $T_{1/2}$ by the condition $\Phi(T_{1/2}) \equiv 1/2$ implies that $K_{p,m}^{(\phi)}(T=T_{1/2})$ equals

$$K_{p,m}^{(\phi)}(T=T_{1/2}) = \frac{1}{(\phi_1^0/2)^{m-1}}. \tag{33}$$

Alternatively, the same condition $\Phi \equiv 1/2$ may be employed to define the critical self-assembly concentration $(\phi_1^0)_{1/2}$ at a fixed temperature $T$ as,

$$(\phi_1^0)_{1/2} = \frac{2}{[K_{p,m}^{(\phi)}(T)]^{1/(m-1)}}. \tag{34}$$

Inserting the expression from Eq. (34) into Eq. (32) generates a simple relation between $\Phi$ and the reduced concentration $\phi_r \equiv \phi_1^0/(\phi_1^0)_{1/2}$,

$$\frac{\Phi}{(1-\Phi)^m} = (2\phi_r)^{m-1}, \tag{35}$$

that is valid for arbitrary $m \geqslant 2$. Thus, plotting $\Phi$ vs $\phi_r$ produces for a given $m \geqslant 2$ a universal curve for all tempera-

tures. Setting $m=2$ in Eq. (35) converts the latter into the simple form,

$$\frac{\Phi}{(1-\Phi)^2} = 2\phi_r, \quad m = 2.$$

Equation (35) coincides with a relation noted by Kegel.[8]

The practical importance of Eq. (32) becomes clear upon taking the logarithm of both sides of the equation and differentiating with respect of temperature $T$ at fixed $\phi_1^0$ to thereby obtain

$$\frac{d \ln K_{p,m}^{(\phi)}}{dT} = 2(m+1)\frac{d\Phi}{dT}. \tag{36}$$

Since the derivative of the left hand side of Eq. (36) is simply $\Delta h_{p,m}/(k_B T^2)$ [see Eqs. (5) and (31)] and $\Delta h_{p,m} = (m-1)\Delta h_p$, Eq. (36) then reduces to

$$\frac{\Delta h_p}{k_B T}(m-1) = 2(m+1)T\frac{d\Phi}{dT}, \tag{37}$$

which provides a means of independent determining the cooperativity factor $m$ when $\Delta h_p$ and $\Phi(T)$ are known. The extent of polymerization $\Phi(T)$ is a common observable, while the "sticking energy" $\Delta h_p$ is related to the temperature variation of $(\phi_1^0)_{1/2}$ as

$$\Delta h_p = k_B T_{1/2}^2 \left.\frac{d \ln(\phi_1^0)_{1/2}}{dT}\right|_{T=T_{1/2}}. \tag{38}$$

Equation (38), however, strictly applies only to the $\mathcal{FA}m$ and $\mathcal{FA}$ models.

### D. Simplified models of cooperative transitions

It is frequently assumed for mathematical simplicity that self-assembly can be described abstractly as a "unimolecular" transition between a disordered state $A$ and an ordered state $B$ (i.e., as a transition in which cooperativity is not overtly emphasized),

$$A \rightleftharpoons B. \tag{39}$$

Consequently, the order parameter $\Phi$ (defined as the fraction of A that is converted to B) is expressed in the simple form,

$$\Phi = \frac{1}{1+\exp[(\Delta h - T\Delta s)/(k_B T)]}, \tag{40}$$

where $\Delta h$ and $\Delta s$ are the enthalpy and entropy associated with the reaction in Eq. (39).[52] Equation (40) is popular in modeling the assembly of nanoparticles mediated by DNA hybridization interactions[53] and the thermodynamic "excitations" in glass-forming liquids.[54] The analytic expression in Eq. (40) for $\Phi$ is commonly simplified even further by defining the transition temperature $T_p$ as $T_p \approx \Delta h/\Delta s$ and then expanding the arguments in the exponential of Eq. (40) about $T_p$ to produce the popular "Fermi-function" approximation,[53]

$$\Phi \approx \frac{1}{1+\exp[-\Delta h(T-T_p)/(k_B T_p^2)]} \equiv \frac{1}{1+\exp[(T-T_p)/D_0]}, \tag{41}$$

where $D_0 \equiv k_B T_p^2/|\Delta h|$ reflects the "width" of the self-assembly transition [$D_0$ is the analog of $D$ in Eq. (44) below]. The approximate Eq. (41) has been used, for instance, to treat the main gel-liquid transition in lipid films where the "number of cooperative units" $m$ in the transition is estimated by combining the fitting of $D_0$ to experimental data for $\Phi(T)$ with the experimental determination of the calorimetric enthalpy $\Delta h_{\rm cal}$ for the ordering process,[55,56] by assuming the validity of the relationship,[56,57]

$$\Delta h_{\rm cal} m \equiv (k_B T_p^2)/D_0, \tag{42}$$

which frankly cannot be consistently derived from the two-state model. Given the numerous assumptions involved in determining $m$ by this procedure, the corresponding values of $m$ should not be taken too literally, although the tabulated estimates of $m$ provide a measure of the relative slope of $\Phi$ near the transition temperature, i.e., the transition sharpness.

## III. ANALYSIS OF SIMILARITIES BETWEEN $\mathcal{FA}m$ AND $\mathcal{A}$ MODELS

While Eqs. (10)–(29) generally apply to equilibrium self-assembly phenomenon occuring either upon cooling or heating, our illustrative calculations and discussion below refer to the former case for brevity, corresponding to the assumption that both $\Delta h_p$ and $\Delta s_p$ are negative. These two free energy parameters are chosen to be the same as those employed in our previous studies (i.e., $\Delta h_p = -35$ kJ/mol and $\Delta s_p = -105$ J/mol K) and as determined by Greer[58] for equilibrium polymerization of $\alpha$-methyl styrene. In addition, the lattice coordination number $z$ in Eqs. (13) and (14) is assumed to be $z=6$ (appropriate to a cubic lattice), and the stiffness parameter $\alpha$ in the same equations is $(z-1)$. Thus, all associating species are treated as fully flexible entities.

### A. Average degree $L$ of aggregation as a measure of the sharpness of the self-assembly transition

We begin the analysis of the $\mathcal{FA}m$ model by examining the temperature variation of the average degree of polymerization $L$ for several cluster sizes $m$ and for fixed initial monomer concentration $\phi_1^0$ in Fig. 1. As anticipated, $L(T, \phi_1^0 = \text{const})$ achieves a low temperature plateau $L_p = m$ for the $\mathcal{FA}m$ model, but $L$ gradually diminishes to unity at sufficiently high temperatures where association is absent, and, consequently, where the $\mathcal{FA}m$ system consists only of monomers $M_1$ and solvent molecules. The behavior of $L(T)$ for the $\mathcal{FA}m$ model in Fig. 1 sharply contrasts with the unlimited growth in $L(T)$ at low temperatures for the $\mathcal{FA}$ model. The $L(T)$ curves for the $\mathcal{FA}m$ model in Fig. 1 *resemble* the temperature variation of $L(\phi_1^0 = \text{const})$ for both the chemically initiated equilibrium polymerization $\mathcal{I}$ model[42] and the activated association $\mathcal{A}$ model[32] when the enthalpies of activation and propagation are *identical* ($\eta \equiv \Delta h_a/\Delta h_p$

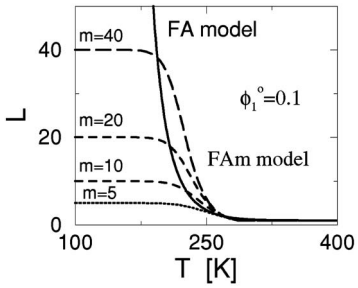


FIG. 1. Average aggregate size $L$ as a function of temperature $T$ for fixed initial monomer concentration $\phi_1^0=0.1$, for the $\mathcal{FA}$ model of equilibrium polymerization, and for a series of $\mathcal{FA}m$ models with varying cluster size $m$. The free energy parameters $\Delta h_p$ and $\Delta s_p$ and the stiffness parameter $\alpha$ are given in the text. The same values of $\Delta h_p$, $\Delta s_p$, and $\alpha$ are used in the calculations illustrated in Figs. 2–13 and 16–19.

$=1$) and when the entropy ratio $\sigma \equiv \Delta s_a/\Delta s_p$ satisfies the condition $\sigma > 1$. Following our previous paper,[32] we term this model the $\mathcal{A}_\sigma$ model. In particular, a low temperature plateau $L_p=\text{const}/r$ emerges[42] for the living polymerization $\mathcal{I}$ model [with $r$ denoting the reduced concentration $\phi_I/\phi_1^0$ of the initiator $I$ and with the constant (const=1 or 2) designating the number of active ends in the initiator molecule], while the magnitude of $L_p$ for the $\mathcal{A}_\sigma$ model depends[32] for fixed initial monomer concentration $\phi_1^0$ only on the entropy difference $(\Delta s_a - \Delta s_p)$.

### B. Extent of association Φ: Universal reduced temperature and concentration variables for self-assembly

The influence of cooperativity on self-assembly is examined further in Figs. 2–5 by comparing the temperature and concentration dependence of the extent of association Φ for the ideally noncooperative $\mathcal{FA}$ model with that for the cooperative $\mathcal{FA}m$ model. Figure 2 displays Φ as a function of temperature $T$ for several fixed cluster sizes $m$ and for the initial concentration $\phi_1^0=0.1$ that is used in Fig. 1 to illustrate $L(T)$. Increasing $m$ leads to a sharper profile for $\Phi(T)$ and consequently to a sharper self-assembly transition. A similar conclusion also emerges from examining the concentration dependence of the order parameter Φ, as illustrated in Fig. 3 for $T=300$ K and several cluster sizes $m$. Figures 4 and 5 further demonstrate that both the temperature and composition dependence of Φ are transformed to essentially

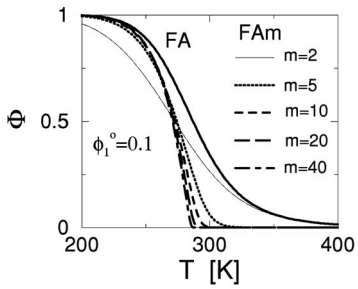


FIG. 2. Extent of association Φ as a function of temperature $T$ for fixed initial monomer concentration $\phi_1^0=0.1$ and for the $\mathcal{FA}m$ model. Different curves correspond to different $m$ in the $\mathcal{FA}m$ model. The $\Phi(T)$ curve for the $\mathcal{FA}$ model is included for comparison.

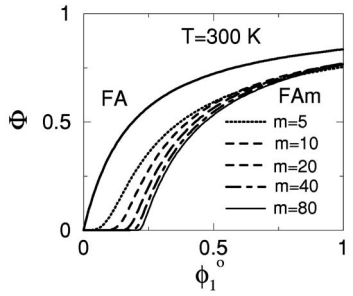


FIG. 3. Extent of association Φ as a function of the initial monomer concentration $\phi_1^0$ at fixed temperature $T=300$ K. Different curves correspond to different $m$ in the $\mathcal{FA}m$ model. The $\Phi(\phi_1^0)$ curve for the $\mathcal{FA}$ model is included for comparison.

*universal* scalings when $T$ and $\phi_1^0$ are normalized by the scaling temperature ($T_{1/2}$, $T_\Phi$, or $T_{C_V}$) and the scaling concentration [$(\phi_1^0)_{1/2}$ for instance], respectively. Although the examples in Figs. 4 and 5 are generated for $m=40$, the reduced variable description applies for all $m \geqslant 2$. Hence, a unique pair of universal curves $\Phi(T/T_{1/2} \equiv T_r)$ and $\Phi(\phi_1^0/(\phi_1^0)_{1/2})$ describes (for each $m$) data for all compositions $\phi_1^0$ and all temperatures $T$, respectively. This universal behavior of self-assembling systems is reminiscent of the corresponding state description for fluid phase separations[59] and even holds for the $\mathcal{FA}$ model whose self-assembly transition is extremely broad.[20,21,60] Thus, the reduced temperature and concentration variables have significance *regardless of the transition broadness*. The same type of universality also applies to the average degree of association $L$, which is simply related to Φ for the $\mathcal{FA}m$ model as,

$$\Phi = \frac{m}{m-1}\frac{L-1}{L}. \tag{43}$$

Equation (43) also establishes the obvious relation between the low and high temperature limits of $L$ and Φ. Specifically, substituting the low temperature limit $L=m$ into Eq. (43) yields $\Phi=1$, i.e., the well-known low temperature limit for the extent of polymerization upon cooling, whereas the use in Eq. (43) of the high temperature limit $L=1$ implies that the fraction Φ of monomers converted into aggregates exactly vanishes.

As already mentioned, the temperature $T_{1/2}$ at which the order parameter is $\Phi=1/2$ is often identified with the

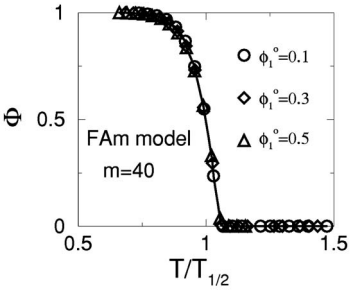


FIG. 4. Extent of association Φ as a function of the reduced temperature $T_r \equiv T/T_{1/2}$ [with $T_{1/2}$ defined by the condition $\Phi(T=T_{1/2}, \phi_1^0)=1/2$] for the $\mathcal{FA}m$ model with $m=40$. Different symbols correspond to the different initial monomer concentrations $\phi_1^0$ specified in the figure. Note that $T_{1/2}$ varies with $\phi_1^0$.

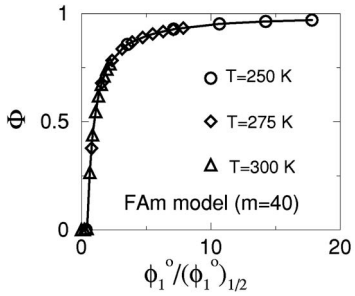


FIG. 5. Extent of association $\Phi$ as a function of the reduced concentration $\phi_r \equiv \phi_1^0/(\phi_1^0)_{1/2}$ [with $(\phi_1^0)_{1/2}$ defined by the condition $\Phi((\phi_1^0)_{1/2},T)=1/2$] for the $\mathcal{FA}m$ model with $m=40$. Different symbols correspond to the different temperatures indicated in the figure. Note that $(\phi_1^0)_{1/2}$ varies with $T$.

self-assembly transition temperature $T_p$. Roughly speaking, for systems that associate upon cooling, monomers of the associating species $M$ are mostly unassociated above $T_p$, while significant clustering ensues below $T_p$ and vice versa for systems that cluster upon heating. Inspection of Fig. 2 also suggests that the derivative $\partial\Phi/\partial T|_{T=T_{1/2}}$ provides a good quantitative measure of the sharpness of the polymerization transition, as illustrated in Fig. 6, which presents $\partial\Phi/\partial T|_{T=T_{1/2}}$ as a function of $\phi_1^0$ for the $\mathcal{FA}m$ model. Indeed, the absolute value of $\partial\Phi/\partial T|_{T=T_{1/2}}$ increases with $m$ for all initial monomer compositions $\phi_1^0$ and exceeds the corresponding values of $|\partial\Phi/\partial T||_{T=T_{1/2}}$ for the $\mathcal{FA}$ model provided that $m$ is greater than 2. The temperature width $D$ of the self-assembly transition is defind as

$$D \equiv 1/|\partial\Phi/\partial T|_{T=T_{1/2}} \tag{44}$$

and is useful in analyses of experimental data for self-assembly. Evidently, the ratio $D/T_{1/2}$ provides a useful dimensionless measure for the breadth and sharpness of the self-assembly transition, a measure that is independent of model assumptions about the detailed nature of the transition. According to Eq. (37), knowledge of the derivative $\partial\Phi/\partial T|_{T=T_{1/2}}$ enables the independent determination of $m$,

$$m = \frac{|\Delta h_p|/(k_B T_{1/2}) + 2T_{1/2}/D}{|\Delta h_p|/(k_B T_{1/2}) - 2T_{1/2}/D}, \tag{45}$$

provided that the enthalpy $\Delta h_p$ is known. [For the $\mathcal{FA}m$ model, $\Delta h_p$ can be estimated from Eq. (38).] Equation (45), thus, offers an opportunity of defining an effective value of $m$ for other models of self-assembly from experimental data

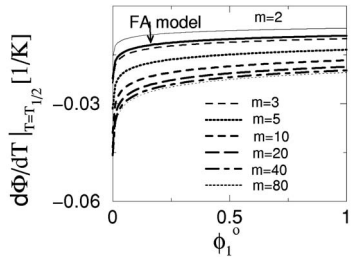


FIG. 6. Derivative $\partial\Phi/\partial T|_{T_{1/2}}$ as a function of the initial monomer concentration $\phi_1^0$ for the $\mathcal{FA}$ model and for a series of $\mathcal{FA}m$ models with varying cluster size $m$.

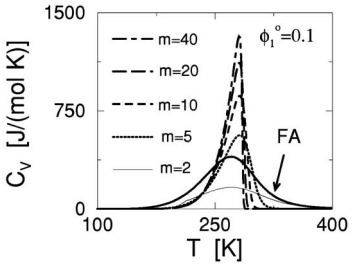


FIG. 7. Specific heat $C_V$ as a function of temperature $T$ at fixed initial monomer concentration $\phi_1^0=0.1$ for the $\mathcal{FA}$ model and for a series $\mathcal{FA}m$ models with varying cluster size $m$.

for $\Phi(T)$. It is worth mentioning that the alternative of choosing $T_\Phi$ as the transition temperature $T_p$, along with the derivative $\partial\Phi/\partial T|_{T=T_\Phi}$ as a function of $\phi_1^0$ for various $m$, leads to the same general trends as those generated from Fig. 6.

### C. Specific heat and nature of self-assembly transition in the high cooperativity limit

The nonvibrational component of the specific heat occupies a special place in the characterization of equilibrium self-assembly solutions because of its utility in estimating $T_p$ and in quantifying the sharpness of the self-assembly transition. Figure 7 displays the specific heat $C_V(T)$ for a fixed concentration $\phi_1^0$ and demonstrates that increasing $m$ leads to a higher maximum, to a sharper peak of $C_V(T)$ for the $\mathcal{FA}m$ model, and thus a "sharper" transition. The temperature variation of $C_V(T)$ for the $m=2$ system indicates that the transition is even *broader* than for the $\mathcal{FA}$ model. The extremely broad transition for $m=2$ contrasts with the case of $m=5000$ presented in Fig. 8. When $m$ becomes large, the self-assembly transition clearly approaches a *second order phase transition*, and the illustrative example of Fig. 8 answers our question (c).

The polymerization transition lines $T_\Phi(\phi_1^0)$ and $T_{C_V}(\phi_1^0)$ (see Fig. 9) augment our understanding of the influence of $m$ on the transition broadness in the $\mathcal{FA}m$ and $\mathcal{A}_\sigma$ models. Our previous studies[19] indicate that while these two characteristic temperatures differ by 20–30 K for the $\mathcal{FA}$ model, they are identical for systems in which the association transition is very sharp. The transition sharpness is controlled by the magnitude of either the equilibrium constant $K_a$ ($\mathcal{A}_\sigma$ model) or the initiator composition $r$ of the initiator ($\mathcal{I}$ model).[42] Since the general trends in thermodynamic properties of the $\mathcal{FA}m$ model more closely resemble those typical of the $\mathcal{A}_\sigma$

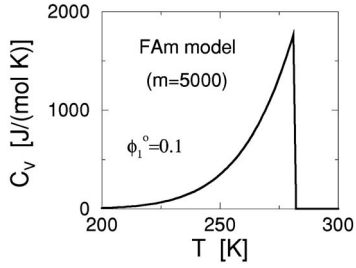


FIG. 8. Specific heat $C_V$ as a function of temperature $T$ at fixed initial monomer concentration $\phi_1^0=0.1$ for the $\mathcal{FA}m$ model with $m=5000$.

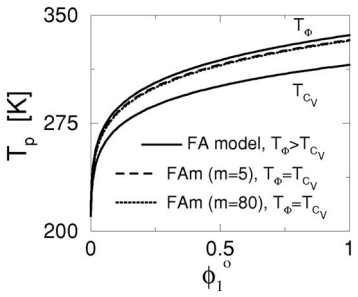


FIG. 9. Polymerization transition temperature $T_p$ as a function of initial monomer concentation $\phi_1^0$ for the $\mathcal{FA}$ and $\mathcal{FA}m$ models. While the temperatures $T_\Phi$ and $T_{C_V}$ (defined in the text) differ for the $\mathcal{FA}$ model, they are identical for the $\mathcal{FA}m$ model, providing a unique defintion of $T_p$.

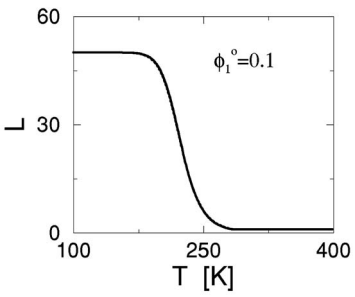


FIG. 11. Comparison of the temperature variation of the average cluster size $L$ for fixed initial monomer concentration $\phi_1^0=0.1$ between the $\mathcal{FA}m$ model with $m=50$ (solid line) and the $\mathcal{A}_\sigma$ model with $\Delta h_a=\Delta h_p=-35\,000$ kJ/mol and $\Delta s_a=-185$ J/mol K (dotted line). These two curves are indistinguishable by the naked eye (the relative difference is less than 1%).

model than those of the $\mathcal{FA}$ model (see Figs. 1–3 and 7 for better visualization), comparison of $T_\Phi$ and $T_{C_V}$ for the $\mathcal{FA}m$ system provides a stringest test of the degree of similarity. Both temperatures are numerically found to be essentially identical for the $\mathcal{FA}m$ model over the whole composition range of $0<\phi_1^0\leqslant 1$, which suggests, in turn, that the similarity between the $\mathcal{FA}m$ and $\mathcal{A}_\sigma$ models is not fortuitous, but rather is based on the existence of a physically meaningful interrelation between the models. Figure 9 exhibits the polymerization lines $T_p(\phi_1^0)$ for several $\mathcal{FA}m$ models with $m$ ranging from $m=2$ to $m=80$. Further increasing $m$ beyond $m=80$ produces almost no changes in $T_p(\phi_1^0)$, so that the polymerization line for $m=80$ also represents $T_p(\phi_1^0)$ in the $m\to\infty$ limit. All polymerization lines for the $\mathcal{FA}m$ system in Fig. 9 (except for $m=2$) lie between the two polymerization lines for the $\mathcal{FA}$ model, i.e., between $T_\Phi(\phi_1^0)$ (the top curve in Fig. 9) and $T_{C_V}(\phi_1^0)$ (bottom curve in Fig. 9). The relation between these models is pursued more quantitatively in Sec. III E.

### D. Regularities in the magnitude of *L* for self-assembly

Complementary information about the equilibrium association transition is often obtained by examining the average degree $L$ of association at the polymerization temperature $T_p$. Figure 10 illustrates $L(T_p)$ as a function of $\phi_1^0$ for the $\mathcal{FA}m$ model with variable $m$. When $m$ increases, $L(T_p)$ approaches unity as long as $m$ is reasonably large. The same trend exists in the $\mathcal{A}_\sigma$ and $\mathcal{I}$ models as the self-assembly transition becomes sharper. Thus, the deviation of $L(T_p)$ from unity [i.e., $L(T_p)-1$] provides a measure of transition rounding similar

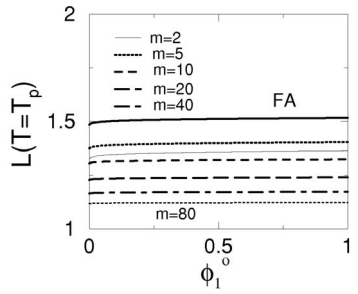


FIG. 10. Average aggregate size $L$ at the polymerization temperature $T_p$ as a function of initial monomer concentration $\phi_1^0$ for the $\mathcal{FA}$ model and for a series of $\mathcal{FA}m$ models with varying $m$.

to that provided by the parameter $\delta_h$ (see Sec. III F). These calculations explain the basic observation[18] that under thermodynamic conditions *near* the self-assembly transition, noncooperative assembly often involves the formation of small clusters, while cooperative assembling essentially produces either monomeric structures or massive polymers.

### E. Quantitative mapping between the $\mathcal{FA}m$ and $\mathcal{A}_\sigma$ models

A quantitative comparison of these two models requires specifying the activation entropy for the $\mathcal{A}_\sigma$ model. The choice of $\Delta s_a=-185$ J/mol K ($\sigma\equiv\Delta s_a/\Delta s_p\approx 1.75$) ensures a relatively sharp polymerization transition, but, as shown below, the precise value of $\Delta s_a$ does not affect the final qualitative conclusions. Figure 11 presents the temperature variation of the average cluster size $L(\phi_1^0=0.1)$ for the $\mathcal{A}_\sigma$ model with identical enthalpies ($\eta\equiv\Delta h_a/\Delta h_p=1$), but different entropies of activation and propagation ($\sigma\approx 1.75$). Setting $m=50$ in the $\mathcal{FA}m$ model leads to $L(\phi_1^0=0.1)$ in the $\mathcal{FA}m$ and $\mathcal{A}_\sigma$ models being identical not only at low temperatures but also essentially at all temperatures. Alternatively, $\Delta s_a$ may be chosen to ensure the superposition of the $L(T,\phi_1^0=0.1)$ curves for these two models. Given the $\mathcal{FA}m$ model with $m=50$, this alternative yields $\Delta s_a\approx -185$ J/mol K, which is consistent with the original value of $\Delta s_a$ used for the calculations in Fig. 11. The quality of reproduction of $L(T)$ for the $\mathcal{A}_\sigma$ model (solid curve in Fig. 11) by $L(T)$ for the $\mathcal{FA}m$ model (dotted curve in Fig. 11) is amazing. In fact, these two curves differ by less than 1%, and the difference decreases with increasing $m$. Further comparisons between the $\mathcal{FA}m$ and $\mathcal{A}_\sigma$ models do not involve adjustable parameters since $m$ is fixed at 50. Figures 12 and 13, thus, demonstrate that all basic thermodynamic quantities, such as the extent of association $\Phi(T)$ and the specific heat $C_V(T)$, are essentially identical for the $\mathcal{A}_\sigma$ and $\mathcal{FA}m$ models. The corresponding values of $m$ for the $\mathcal{FA}m$ model and of $\Delta s_a$ for the $\mathcal{A}_\sigma$ model must clearly be related to ensure the close similarity of the predictions of the two models. Figure 14 provides the values of $m$ value that guarantee the identity of the $L(T,\phi_1^0=\text{const})$ curves for the two models as a function of the initial monomer concentration $\phi_1^0$ for a few choices of the activation entropy $\Delta s_a$. Evidently, increasing $|\Delta s_a|$ (i.e., considering a

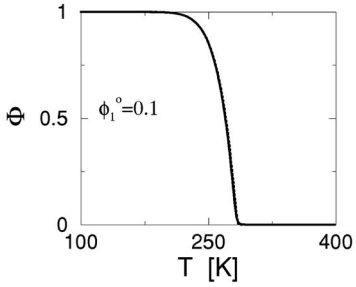


FIG. 12. Comparison of the temperature variation of the extent of association $\Phi$ for fixed initial monomer concentration $\phi_1^0=0.1$ between the $m$ model with $m=50$ (solid line) and the $\mathcal{A}_\sigma$ model with $\Delta h_a=\Delta h_p=-35\,000$ kJ/mol and $\Delta s_a=-185$ J/mol K (dotted line). These two curves are hardly distinguishable by the naked eye (the highest relative difference is about 4%).

sharper self-assembly transition) leads to a larger $m$. Thus, the $m\to\infty$ limit of the $\mathcal{FA}m$ model corresponds to the $K_a\to 0$ limit in the $\mathcal{A}_\sigma$ model, where the transition is already known to be of second order.[61,62] The fitted $m$ becomes more sensitive to $\phi_1^0$ with increasing $|\Delta s_a|$. For instance, if $\sigma\equiv\Delta s_a/\Delta s_p=3$ [which implies $K_a\sim\mathcal{O}(10^{-8}-10^{-11})$ for $200\ \mathrm{K}<T<300\ \mathrm{K}$], the corresponding $m$ for the $\mathcal{FA}m$ model and $\phi_1^0=1$ (found by using the same procedure illustrated in Fig. 11) is extremely large ($m\approx 4\times 10^5$).

### F. Measures of transition cooperativity and transition rounding

While Eq. (45) has been derived for the $\mathcal{FA}m$ model, it can be used as a definition of the cooperativity parameter $m$ for other models of self-assembly, provided that the propagation enthalpy $\Delta h_p$, the polymerization temperature $T_{1/2}$, and the width $D\equiv 1/|\partial\Phi/\partial T|_{T=T_{1/2}}$ of transition are known for these models. The resulting $m$ is denoted as $m_{\mathrm{eff}}$ in order to distinguish from the parameter $m$ of the $\mathcal{FA}m$ model. The derivative $\partial\Phi/\partial T|_{\phi_1^0}$ has the simple analytical form

$$\left.\frac{\partial\Phi}{\partial T}\right|_{\phi_1^0}=\left[\frac{1}{\phi_1^0 T(1-A)^3\phi_1^0+2CA^2}\frac{2CA^2\phi_1}{}\right]\frac{\Delta h_p}{k_BT}, \tag{46}$$

$\mathcal{FA}$ model,

and

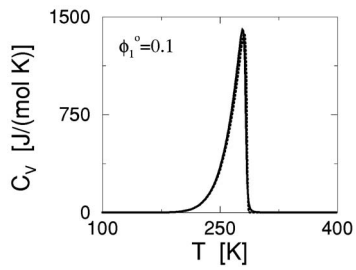


FIG. 13. Comparison of the temperature variation of the specific heat $C_V$ for fixed initial monomer concentration $\phi_1^0=0.1$ between the $\mathcal{FA}m$ model with $m=50$ (solid line) and the $\mathcal{A}_\sigma$ model with $\Delta h_a=\Delta h_p=-35\,000$ kJ/mol and $\Delta s_a=-185$ J/mol K (dotted line). These two curves are hardly distinguishable by the naked eye (the highest relative difference is about 6%).

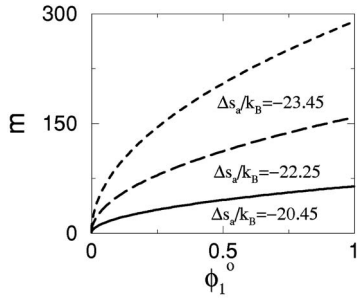


FIG. 14. Cooperativity index $m$ as a function of the initial monomer concentration $\phi_1^0$, obtained by demanding the superposition of the temperature variation of average aggregate size $L$ for the $\mathcal{FA}m$ and $\mathcal{A}_\sigma$ models. Different curves correspond to the indicated entropies of activation $\Delta s_a$ for the $\mathcal{A}_\sigma$ model.

$$\left.\frac{\partial\Phi}{\partial T}\right|_{\phi_1^0}=\left[\frac{1}{\phi_1^0 T\left(\phi_1^0+\dfrac{2CA^2}{(1-A)^3}\right)}\right]\left[\frac{2CA^2\phi_1}{(1-A)^3}\frac{\Delta h_p}{k_BT}+\frac{2CA^2(2-A)\phi_1}{(1-A)^2}\frac{\Delta h_a}{k_BT}\right], \tag{47}$$

$\mathcal{A}_\sigma$ model.

Equations (44)–(47), in conjuction with Eq. (22), then enable the determination of $T_{1/2}$ and estimation of $m_{\mathrm{eff}}$. Table I summarizes illustrative calculations of $T_{1/2}$, $D$, $m_{\mathrm{eff}}$, and $L_p$ for the $\mathcal{A}_\sigma$ model when the initial monomer concentration is chosen as $\phi_1^0=0.1$. Increasing the absolute value of $\Delta s_a$ (i.e., the sharpness of the transition) leads to a diminished $D$ and a larger $m_{\mathrm{eff}}$. The latter quantity only qualitatively tracks $L_p$, the average cluster size $L$ in the low temperature limit. Evidently, Eq. (45) only provides a rough estimate of the cooperativity index as the size of assembly at low temperatures. On the other hand, $m_{\mathrm{eff}}$ remains a good measure of how

TABLE I. The polymerization temperature $T_{1/2}$, the transition width $D$, the effective cooperativity index $m_{\mathrm{eff}}$, and the low temperature limit $L_p$ of the average cluster size $L$ for the $\mathcal{A}_\sigma$ model of equilibrium self-assembly analyzed in the text. The properties considered are presented as functions of the ratio $\sigma\equiv\Delta s_a/\Delta s_p$, where the entropy of activation $\Delta s_a$ varies and the entropy of propagation $\Delta s_p$ is fixed as −105 J/mol K.

| $\Delta s_a$ (J/mol K) | $\sigma\equiv\Delta s_a/\Delta s_p$ | $T_{1/2}$ (K) | $D$ (K) | $m_{\mathrm{eff}}$ | $L_p$ |
|---|---|---|---|---|---|
| −115[a] | 1.10 | 295.18 | 218.8 | 1.5 | 1.2 |
| −125[a] | 1.19 | 282.75 | 91.73 | 2.4 | 1.6 |
| −135[a] | 1.29 | 276.89 | 56.01 | 4.7 | 2.6 |
| −145[a] | 1.38 | 273.88 | 43.89 | 9.7 | 4.5 |
| −155[a] | 1.48 | 272.05 | 38.99 | 19.4 | 8.2 |
| −165[a] | 1.57 | 270.93 | 36.77 | 37.9 | 15 |
| −175 | 1.67 | 270.24 | 35.73 | 68.1 | 27 |
| −185 | 1.76 | 269.89 | 35.13 | 133 | 50 |
| −195 | 1.86 | 269.68 | 34.84 | 245 | 91 |
| −205 | 1.95 | 269.57 | 34.67 | 489 | 167 |
| −215 | 2.05 | 269.50 | 34.59 | 832 | 304 |
| −225 | 2.14 | 269.47 | 34.54 | 1553 | 556 |
| −235 | 2.24 | 269.45 | 34.52 | 2766 | 1014 |
| −245 | 2.33 | 269.44 | 34.50 | 5588 | 1850 |

[a]Because $\Phi$ saturates at low temperatures to a constant $c<1$, the temperature $T_{1/2}$ corresponds to the temperature at which $\Phi=c/2$.

closely the transition approaches a phase transition. A meaningful result for $m_{\rm eff}$ is obtained even for the uncooperative $\mathcal{FA}$ model, where we find that $m_{\rm eff}=3.0$ regardless of the initial monomer concentrations $\phi_1^0$ and that $m_{\rm eff}$ is entirely insensitive to the magnitudes of $\Delta s_p$ and $\Delta h_p$. Deviation of $m_{\rm eff}$ from 3 then provides a quantitative measure of the "extent of transition cooperativity."

Numerous other measures of "cooperativity" are commonly reported in the literature.[39,40,63] For instance, transition "thermodynamic cooperativity"[63] is often specified in terms of the ratio $\kappa_h$,

$$\kappa_h \equiv \frac{\Delta h_{\rm vH}}{\Delta h_{\rm cal}}, \tag{48}$$

where $\Delta h_{\rm vH}$ denotes the van't Hoff enthalpy and $\Delta h_{\rm cal} \equiv \int_{T_1}^{T_2}(C_P - C_P^{(\rm vib)})dT$ is the excess enthalpy (determined calorimetrically) with $T_1$ and $T_2$ designating the temperatures at which the specific heat $C_P - C_P^{(\rm vib)}$ approaches zero, respectively, and where $C_P^{(\rm vib)}$ denotes the vibrational contribution to the specific heat $C_P(T)$. The van't Hoff enthalpy $\Delta h_{\rm vH}$ is operationally defined by Eq. (27) and is determined from measurements of the concentration dependence of the polymerization (self-assembly) temperature $T_p$. (Frequently, $T_p$ is identified with the temperature at which the specific heat achieves the maximum, but the different methods of estimating $T_p$ normally yield essentially the same value of the self-assembly transition temperature, provided the transition is reasonably sharp.[59]) At first glance, the parameter $\kappa_h$ of Eq. (38) seems to be a highly attractive choice as a metric for transition cooperativity, since it is specified in terms of directly observable quantities ($\Delta h_{\rm vH}$ and $\Delta h_{\rm cal}$). However, an examination of these quantities in the perfectly uncooperative $\mathcal{FA}$ model (see below) reveals that $\kappa_h$ significantly varies with the entropy of self-assembly $\Delta s_p$. Thus, $\kappa_h$ must be rejected as solely a measure of transition cooperativity.

On the other hand, transition rounding is an essential aspect of self-assembly that is certainly influenced by cooperativity, and this property of self-assembly also requires quantification. For this purpose, we introduce the related ratio $\delta_h$,

$$\delta_h \equiv \Delta h_{\rm vH}/\Delta h_p, \tag{49}$$

which differs from the definition of $\kappa_h$ only by normalization [i.e., the true propagation enthalpy $\Delta h_p$ is used in Eq. (49) instead of the calorimetric excess enthalpy $\Delta h_{\rm cal}$]. Note that for the $\mathcal{FA}$ and $\mathcal{A}_\sigma$ models, $\delta_h$ and $\kappa_h$ can be shown to be identical, but the relation between these quantities is generally not so simple. The ratio $\delta_h$ has a clear interpretation as the extent to which transition rounding modifies (*renormalizes*) the effective enthalpy[64] of assembly. Given the definition of $\Delta h_{\rm vH}$, $\delta_h$ of Eq. (49) is termed the *enthalpy renormalization parameter*, and we discuss the dependence of $\delta_h$ on cooperativity and other factors that influence the sharpness of the self-assembly transition below. The enthalpy renormalization parameter $\delta_h$ has been previously analyzed by Van Workum and Douglas[21] for the Stockmayer fluid and a real system of associating dipolar particles,[60] where $\delta_h$ is found to substantially deviate from unity and to accord well with our prediction for the $\mathcal{FA}$ model (see below).

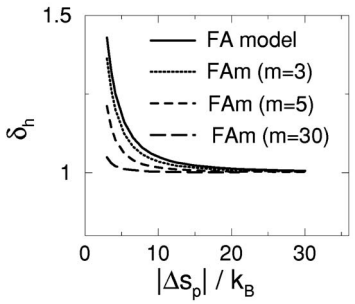


FIG. 15. The ratio $\delta_h \equiv \Delta h_{\rm vH}/\Delta h_p$ of the van't Hoff enthalpy $\Delta h_{\rm vH}$ and the enthalpy of propagation $\Delta h_p$ as a function of the entropy of propagation $\Delta s_p$ for a series of $\mathcal{FA}m$ models (with varying cluster size $m$) and for the perfectly "uncooperative" $\mathcal{FA}m$ model. The parameter $\delta_h$ is completely insensitive to the enthalpy of propagation $\Delta h_p$. The polymerization line $T_p = T_p(\phi_1^0)$ used to estimate $\Delta h_{\rm vH}$ (see the text for more details) is determined from the maximum in the specific heat $C_V(T)$, based on Eqs. (23) and (24).

The evaluation of $\Delta h_{\rm vH}$ requires fitting the computed polymerization line $T_p = T_p(\phi_1^0)$ [where $T_p$ corresponds to the temperature at which the specific heat $C_V(T)$ achieves a maximum] by Eq. (27). Specifically, the van't Hoff enthalpy ($\Delta h_{\rm vH}$) is normally experimentally obtained by plotting the logarithm of the critical polymerization concentration $\phi_1^0$ (defined by the polymerization transition line) versus $1/T$. Following this procedure, the relative deviation between $T_p$ obtained from Eq. (27) and $T_p$ evaluted from the analytical expression for $C_V$ is generally less than a few percent in the concentration range from $\phi_1^0=0.1$ to $\phi_1^0=1$. Knowledgle of $\Delta h_{\rm vH}$ then enables evaluating $\delta_h$. Figure 15 demonstrates that $\delta_h$ monotonically decreases with increasing $\Delta s_p$ for both the $\mathcal{FA}$ and $\mathcal{FA}m$ models. This variation is completely insensitive to the enthalpy $\Delta h_p$ of assembly and characterizes (for the $\mathcal{FA}$ model) the extent of the drop of the (nonvibrational) entropy upon passing through the self-assembly transition, a drop that is directly proportional to $\Delta s_p$.[65] The curve of $\delta_h = \delta_h(\Delta s_p)$ for the $\mathcal{FA}m$ model with $m=3$ is very similar to that for the $\mathcal{FA}$ model, which is consistent with our finding of $m_{\rm eff}=3$ for the $\mathcal{FA}$ model above. The dependence of $\delta_h$ for the $\mathcal{FA}$ model on $\Delta s_p$ indicates that $\delta_h$ and the related $\kappa_h$ are not really direct measures of cooperativity. However, Fig. 15 indicates that changes in the cooperativity index $m$

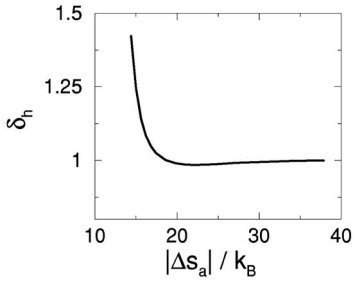


FIG. 16. The ratio $\delta_h \equiv \Delta h_{\rm vH}/\Delta h_p$ of the van't Hoff enthalpy $\Delta h_{\rm vH}$ and the enthalpy of propagation $\Delta h_p$ as a function of the entropy of activation $\Delta s_a$ for the $\mathcal{A}_\sigma$ model. The parameter $\delta_h$ is completely insensitive to the enthalpy of propagation $\Delta h_p$, which coincides with the enthalpy of activation $\Delta h_a$ for the $\mathcal{A}_\sigma$ model. The polymerization line $T_p = T_p(\phi_1^0)$ used to estimate $\Delta h_{\rm vH}$ (see the text for more details) is determined from the maximum of the specific heat $C_V(T)$ computed by using Eq. (25).

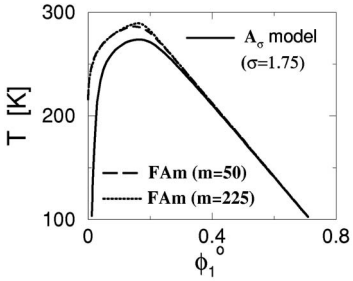


FIG. 17. Comparison of the spinodal curves between the $\mathcal{FA}m$ model with $m=50$ (dashed curve) and the $\mathcal{A}_\sigma$ model ($\Delta s_a=-185$ J/mol K) for which the $L(T,\phi_1^0=0.1)$ curves are identical (see Fig. 11). The spinodal for the $\mathcal{FA}m$ model is computed by using a common $m=50$ for all compositions. The additional spinodal curves for the $\mathcal{FA}m$ model (with $m=225$) illustrate that changing $m$ does not remove discrepancies between the spinodal curves for the two models in the low concentration regime.

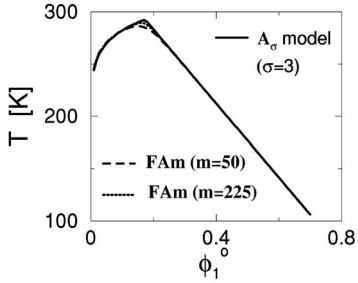


FIG. 18. Comparison of the spinodal curves between the $\mathcal{FA}m$ model with $m=50$ (dashed curve) and the $\mathcal{A}_\sigma$ model ($\Delta s_a=-315$ J/mol K) for which the self-assembly transition resembles a second order transition.

for the $\mathcal{FA}m$ model imply changes in $\delta_h$. For completeness, Fig. 16 illustrates how $\delta_h$ varies with transition sharpness ($\Delta s_a$) for the physically more realistic $\mathcal{A}_\sigma$ model where the *effective* cooperativity index is variable. Figure 16 exhibits that increasing $\Delta s_a$ causes $\delta_h$ to approach unity.

The parameter $\delta_h$ (and $\kappa_h$ of course) clearly depends on transition cooperativity and within a prescribed family of self-assembly models informs about the degree of assembly cooperativity, even though $\delta_h$ cannot generally be used for this purpose. Table I contains the values of $m_{\text{eff}}$, corresponding to the data presented in Fig. 16, and demonstrates that as $m_{\text{eff}}$ increases, the width $D$ of the transition decreases. However, this trend in $D$ saturates at large $m$, so that $D$ cannot really be used to reliably estimate transition cooperativity. Figure 16, in conjunction with Table I, thus indicates that $\delta_h$ monotonically varies with $m_{\text{eff}}$, approaching unity in the $m_{\text{eff}}\to\infty$ limit.

Self-assembly processes do not always lead to the saturation of the average cluster size $L$ to a constant at low temperatures where aggregation occurs with negative entropy and enthalpy changes. For example, $L$ approaches infinity in the $T\to 0$ limit for the $\mathcal{A}$ model when $\eta\equiv\Delta h_a/\Delta h_p>1$. The self-assembly transition from such "open" association models, in which infinite polymers form, can exhibit a variable degree of transition cooperativity, despite the lack of saturation in the cluster growth at low temperatures. Equation (45) still defines an effective $m$ for these models since the width $D$ of the self-assembly transition can be expressed in terms of the derivative $\partial\Phi/\partial T$ evaluated at a particular temperature, such as $T_{1/2}$, and hence $m_{\text{eff}}$ simply quantifies the extent to which the self-assembly approaches a phase transition. Likewise, the definition of $\delta_h$ from Eq. (49) may also be extended to quantify transition rounding in these models. Thus, transition cooperativity is more generally defined by the degree to which thermodynamic transition approaches a true phase transition, and $m_{\text{eff}}$ provides a metric for the "extent of cooperativity."

### G. Phase boundaries in the $\mathcal{FA}m$ and $\mathcal{A}_\sigma$ models

While the formal mapping between the $\mathcal{A}_\sigma$ and $\mathcal{FA}m$ models holds rather well for several properties, such as $L$, $\Phi$, or $C_V$, the phase diagrams display differences. Figure 17 presents the spinodal curves for the "equivalent" $\mathcal{FA}m$ and $\mathcal{A}_\sigma$ models based on comparisons of $L(T)$, $\Phi(T)$, and $C_V(T)$ in Figs. 11–13 for $m=50$ ($\mathcal{FA}m$ model) and $\sigma\approx 1.75$ ($\mathcal{A}_\sigma$ model). While both models exhibit asymmetric phase diagram for a solution of associating species, the spinodal curves of Fig. 17 are only qualitatively similar, with the main differences appearing for small concentrations ($\phi_1^0<0.25$). Generally different phase boundaries for the $\mathcal{FA}m$ and $\mathcal{A}_\sigma$ models result from the following reasons. In contrast to $L$, $\Phi$, or $C_V$, the phase boundaries depend on the size distribution of the aggregates. The cluster size distribution of the $\mathcal{FA}m$ model at any temperature $T$ and composition $\phi_1^0$ involves only two species, the assembled $m$-clusters, and unassembled monomers, whereas clusters of all possible sizes coexist in the $\mathcal{A}_\sigma$ model, provided the transition is not very sharp. The entropy $\Delta s_a$ in the $\mathcal{A}_\sigma$ model is chosen in Fig. 18 to yield an extremely sharp transition (i.e., resembling a second order transition), improving the agrement between the $\mathcal{FA}m$ and $\mathcal{A}_\sigma$ spinodal curves for high $m$.

## IV. SOME BASIC ASPECTS OF COOPERATIVE SELF-ASSEMBLY

Although some insight into the physical origin of the cooperativity index $m$ emerges from comparing the $\mathcal{FA}m$ and $\mathcal{A}_\sigma$ models, the correspondence *does not* provide a general explanation of cooperativity in self-assembly. While these models illustrate that the presence of thermal activation or chemical initiation in the self-assembly process can modify the sharpness of the self-assembly transition compared to that predicted by the $\mathcal{FA}$ model, many other constraints on the self-assembly process can effectively act in this fashion (see Discussion). The definitions of the cooperativity index $m$ and transition rounding parameter $\delta_h$ presented in the previous section may also be employed to these other models of self-assembly that include conditions on the self-assembly process, such as thermal activation, chemical initiation, elasticity effects, etc. (see Discussion), that modify the thermodynamics from perfectly uncooperative self-assembly, as epitomized by the $\mathcal{FA}$ model. The constraints acting on the self-assembly process can often be quite subtle and difficult to recognize and explain *a priori* in terms of the bare intermolecular interactions for a given self-assembling system. We next describe experimental signatures that serve to identify the presence of cooperativity in self-assembly and

that illustrate the implications of cooperativity on the thermodynamics and kinetics of self-assembly.

### A. Signatures of sharp cooperative transitions in osmotic and transport properties

When the self-assembly transition is highly cooperative (large $m$), as micellization tends to be, the species present at equilibrium are either monomers or clusters of a specific "selected" size $m$, with a small population of structures of intermediate sizes. The population switch between monomers and clusters sharply occurs[18] near the assembly transition, justifying the common use of terms, such as the "critical assembly concentration," "critical gelation concentration," and "critical assembly temperature." Consequently, whenever sharp behavior is observed, cooperativity is implicated, and the remaining issues involve determining the kinds of constraints controlling the self-assembly process. For instance, the micellization transition directly reveals itself in the behavior of the osmotic pressure and more prominently in the osmotic compressibility.[66–72] The same thermodynamic features (e.g., a kink in the concentration dependence of the osmotic pressure, and a corresponding extremum in the concentration dependence of the osmotic compressibility, respectively)[66–72] are also characteristic of highly cooperative transitions, regardless of the physical mechanism responsible for the cooperativity. Our previous papers discuss these properties for the $\mathcal{I}$ and $\mathcal{A}_\sigma$ models,[42,32] so that the details are not repeated. The large $m$ behavior of the $\mathcal{FA}m$ model leads to essentially the same $L(T)$, $\Phi(T)$, and $C_V(T)$ curves as found in our previous studies of these properties in the $\mathcal{I}$ and $\mathcal{A}_\sigma$ models. Experimental data for the collective diffusion coefficient, sedimentation coefficient, electrical conductivity, Soret coefficient,[73] and other basic solution transport properties often exhibit sharp changes in their variation with temperature and composition[2,70] (associated with the sharp changes in the osmotic pressure and isothermal osmotic compressibility on which these transport properties directly depend) that enable the location of the self-assembly transition,[59] provided the data cover a sufficient range of thermodynamic conditions. Notably, these singular thermodynamic features are absent from the $\mathcal{FA}$ model since this model lacks cooperativity by definition. Unfortunately, the idealized $\mathcal{FA}m$ model *fails* to capture the often observed kink in the osmotic pressure and the extremum in the osmotic compressibility that are found for real cooperatively assembling fluids.[74,59] This difficiency of the idealized $\mathcal{FA}m$ model can be traced generally to the insensitivity of the second and third virial coefficients ($A_2$ and $A_3$) to the free energy parameters $\Delta h_p$ and $\Delta s_p$ of self-assembly in the $\mathcal{FA}m$ model because of the lack of a cluster size distribution and, in particular, from the absence of dimers and trimers in the $\mathcal{FA}m$ system when $m>3$. No such difficulty arises in the $\mathcal{A}_\sigma$ model, and these interesting many-body effects on solution properties of cooperatively assembling fluids are discussed in a recent paper.[59]

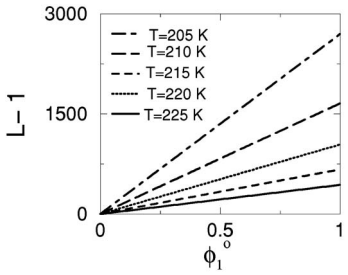


FIG. 19. Composition variation of the average cluster size $L-1$ at fixed temperature for the $\mathcal{A}_\sigma$ model. The different curves correspond to the temperatures indicated in the figure. The same linear variation of $L-1$ with $\phi_1^0$ is obtained for the $\mathcal{FA}m$ model ($m=39\,500$).

### B. Concentration dependence of $L$ as an indicator of cooperativity

It is not widely appreciated that cooperativity also *qualitatively* impacts the dependence of the average mass (or polymerization index $L$) of the self-assembled structures on the initial concentration $\phi_1^0$ of the associating species and temperature $T$. Many mean field treatments of equilibrium polymerization[17,75–77] apply to the $\mathcal{FA}$ model and, for example, predict that the average size $L$ of the aggregates grows as the square root of the initial monomer concentration $\phi_1^0$, i.e., as $L\approx\alpha_L(\phi_1^0)^{1/2}$, where the scaling factor $\alpha_L$ exhibits a nearly Arrhenius temperature dependence,

$$\alpha_L \approx \exp[-\Delta h_p/(2k_BT)]. \tag{50}$$

On the other hand, the presence of an initiator (or thermal activation) qualitatively changes the character of self-assembly,[19,42] such that $L(\phi_1^0)$ at constant temperature $T$ is remarkably linear $L\approx 1+\alpha_L\phi_1^0$, with the factor $\alpha_L$ still represented by an Arrhenius function as in Eq. (50), but with an exponent larger by a factor of 2.[42] A nearly linear concentration dependence for $L$ has been found for nonionic wormlike micelle forming liquids[78,79] and for other associating particle systems.[80] This larger concentration scaling exponent also emerges from calculations of $L$ for the $\mathcal{A}_\sigma$ model (see below) and from simulations of the assembly of nanoparticles in a polymer melt where the self-assembly process derives from the polymer-mediated many-body interactions associated with the polymer matrix.[81]

The linear concentration scaling $L\approx 1+\alpha_L\phi_1^0$ over a large range of temperatures is a general consequence of transition cooperativity, as is now illustrated. Figure 19 exhibits a quite linear concentration dependence of $L$ for the $\mathcal{A}_\sigma$ model ($\sigma=3$) over a wide range of temperatures, and the same $L(\phi_1^0)$ curves are recovered from the the $\mathcal{FA}m$ model by using $m=4\times10^5$ for all $\phi_1^0$. All temperatures in Fig. 19 lie well below the self-assembly temperature $T_p$. Importantly, all curves in Fig. 19 can be superimposed into a common universal curve when $L-1$ is plotted against the ratio $\phi_r \equiv \phi_1^0/(\phi_1^0)_{1/2}$. Figure 20 presents the logarithm of the coefficient $\alpha_L(T)$ in the expression $L=1+\alpha_L(T)\phi_1^0$ as a function of the reciprocal temperature $T^{-1}$ and indicates that $L$ displays an Arrhenius behavior. The values of $\Delta h_p$ deduced from the slopes in Fig. 20 are −34.9 and −34.8 kJ/mol for the $\mathcal{A}_\sigma$ and $\mathcal{FA}m$ models ($m\approx4\times10^5$), respectively, and agree reason-

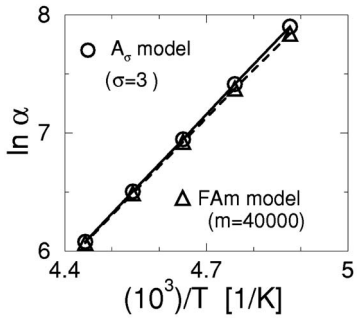


FIG. 20. The logarithm of the factor $\alpha_L$ describing the concentration dependence of $L$ ($L \approx 1+\alpha_L \phi_1^0$) as a function of inverse temperature $1/T$ for the $\mathcal{FA}m$ model ($m \approx 4\times 10^5$) and the $\mathcal{A}_\sigma$ model ($\Delta s_a = -315$ J/mol K).

ably well with the enthalpy of assembly $\Delta h_p = -35$ kJ/mol used in the calculations. This linear variation of $L$ with $\phi_1^0$ is evidently symptomatic of a cooperative assembly, and the determination of $\alpha_L(T)$ provides an attractive means for estimating the enthalpy of propagation for self-assembly processes. Cooperativity qualitatively alters the concentration dependence from the predictions of the simplified noncooperative $\mathcal{FA}$ model.

### C. Signatures of cooperativity from the phase boundaries of self-assembling systems

Our previous paper[32] describes the critical properties of model associating fluids in some detail, and the discussion below focuses on the impact of cooperativity on these properties. In the idealized uncooperative $\mathcal{FA}$ model, an increase of the associative interaction $\Delta h_p$ (relative to the strength $\epsilon_{\mathrm{FH}}$ of the van der Waals interactions) leads to a progressive growth of the magnitude of the cluster size $L$ at the critical point (i.e., $L_c$) for phase separation. Correspondingly, the phase boundaries resemble those of ordinary polymer solutions with a progressively increasing molar mass of the polymers.[32] As $\Delta h_p/\epsilon$ grows, the critical temperature $T_c$ approaches the theta temperature (at which the second virial coefficient $A_2$ vanishes), while the critical composition $\phi_c \equiv (\phi_1^0)_c$ shifts toward zero. These critical properties exhibit more complicated behavior in cooperative assembly models,[32] such as the $\mathcal{A}_\sigma$ and $\mathcal{I}$ models, due to the tendency of $L$ to saturate to a finite low temperatures limit, a feature that also causes the critical composition to achieve a low temperature limit that is related to the limited size of clusters that form at low temperatures.[32] This "pinning" of the magnitude of the critical composition to a fixed value, independent of the strength of interactions, has been observed in both polyelectrolyte simulations[82] and in model water soluble polymers [e.g., poly(N-isopropylacrylate)].[83]

Another qualitative change in the critical properties of associating fluids is the emergence of *multiple* critical points under certain thermodynamic conditions.[19] In particular, our calculations[19] indicate that two critical points can occur when $\Delta h_p$ and $\epsilon_{\mathrm{FH}}$ are comparable in magnitude and the self-assembly transition is reasonably sharp. (This phenomenon never appears in the $\mathcal{FA}$ solution regardless of the magnitude of $\Delta h_p/\epsilon_{\mathrm{FH}}$.) Evidence favoring the existence of multiple critical points has been reported for water,[84] and this phenomenon has been suggested to occur for many fluids exhibiting association.[85] Starr and Sciortino[86] have recently observed multiple critical points in simulations of fluids exhibiting multifunctional association, where cooperativity seems to be present (see Discussion).

### D. Unusual trends in the virial coefficients of cooperatively assembling fluids

Another recently discovered singular behavior[59] further illustrates the qualitative implications of the many-body effects arising due to cooperative assembly. The second virial coefficient $A_2$ of nonassociating fluids generally vanishes at a higher temperature than the temperature at which the third virial coefficient $A_3$ becomes zero. This means that the corresponding theta temperatures defined as $T_{\theta 2} \equiv T(A_2=0)$ and $T_{\theta 3} \equiv T(A_3=0)$ satisfy the condition $T_{\theta 2} > T_{\theta 3}$. When the associative interaction is strong, i.e., self-assembly occurs well above the phase boundary for phase separation, then $T_{\theta 3}$ can actually exceed $T_{\theta 2}$. This odd phenomenon implies, loosely speaking, that the average interparticle interaction, as reflected in $A_2$, can be effectively repulsive on average so the particles repel each other, while more than two particles are attracted! The existence of repulsive two-body interactions and attractive many-body interactions has been found in simulations of hydrophobic species, such as methane in water,[87] and this finding has evident consequences for understanding the hydrophobic effect.[88,89] Evidence also exists that this inversion of the vanishing of the second and third virial coefficients is actually common in solutions of highly charged polyelectrolytes,[59] and indeed we expect that this phenomenon (anticipated by de Gennes[90] for polyethylene oxide in water) to be typical for strongly interacting associating fluids.

### E. High cooperativity and the dynamics of self-assembly

Several basic implications of cooperativity for the dynamics of self-assembly are worth mentioning. Equilibrium self-assembled structures grown under cooperative conditions characteristically display an initial lag phase due to the time required for the activation process,[18] and the initiation time typically exhibits random fluctuations that have many practical consequences.[91] The growth lag is absent for noncooperative assembly. Moreover, noncooperatively assembled chain structures tend more readily to attach and break in their interiors rather than only growing from the chain ends. Erickson and co-workers[18] discussed the ramifications of these fundamentally different types of self-assembly for the functioning of biological systems. Van Workum and Douglas[91] analyzed the change from noncooperative to cooperative assembly that can be induced by simply varying the symmetry properties of the intermolecular potentials between the self-assembly particles.

### F. Cooperativity effects on protein folding

The formation of the native state of proteins in aqueous solutions can formally be considered as a self-assembly process in which the associating species are constrained to lie

within the protein chain. The intramolecular and intermolecular interactions include dipolar and hydrogen bonding interactions, which are mediated by solvent induced interactions ("hydrophobic interactions").[92,93] Direct associations are also present between the solvent and certain hydrophilic portions of protein. Hence, it is hardly surprising that the folding and unfolding of native proteins in solution is a highly cooperative self-assembly process describable in a coarse-grained sense by a two-state assembly model formally similar to the $\mathcal{FA}m$ model.[94–97] However, many proposed models of protein folding are essentially non-cooperative, having a character similar to the $\mathcal{FA}$ model, and this observation has prompted efforts to formulate more realistic models of cooperativity that explain the physical origin of the observed cooperativity.[94–97] The parameter $\kappa_h$ of Eq. (48) is frequently invoked to quantify transition cooperativity in this context, but as discussed above, this parameter simply measures abruptness of the transition.[94–97]

Protein folding thermodynamics raises interesting questions about the meaning of the term cooperativity. While this transition involves the association of many units within the molecule, the transition itself is effectively a unimolecular transformation from a denaturated state to a native state, such that the associations within the molecule and the surrounding solvent constrain this transition, resulting in the observed cooperativity. The limit of high cooperativity in this model corresponds to a *first order phase transition*[97] in which $\kappa_h$ becomes *less* than unity due to transition rounding.[97] This example again illustrates that the basic meaning of cooperativity is the extent to which thermodynamic self-assembly transition resembles a true thermodynamic phase transition.

## V. DISCUSSION

Cooperativity is acknowledged to be a fundamental aspect in many self-assembling systems and glass-forming liquids,[98,99] but this property has usually been treated in an intuitive fashion, leading to some ambiguity in the nature and physical significance of this phenomenon. We, therefore, investigate specific models of self-assembly where the phenomenon naturally arises through the presence of nonlocal constraints (e.g., thermal activation, chemical initiation, formally constrained reaction order) on the self-assembly process, in order to better understand the physical meaning of the cooperativity parameter $m$ in the popular closed association ($\mathcal{FA}m$) model of self-assembly. Specifically, we consider the thermally activated and chemically initiated equilibrium polymerization models and compare basic thermodynamic characteristics of these models to those obtained for the cooperative $\mathcal{FA}m$ model and the idealized noncooperative reference $\mathcal{FA}$ model.

Our analysis of cooperativity focuses on a specific model of activated polymer self-assembly ($\mathcal{A}_\sigma$ model) in which the average degree of polymerization $L$ approaches a constant value at low temperatures as in the $\mathcal{FA}m$ model. A precise mapping between these two models is obtained by finding (for a given initial monomer concentration $\phi_1^0$) a pair of the parameters, the cluster size $m$ of the $\mathcal{FA}m$ model, and the activation entropy $\Delta s_a$ of the $\mathcal{A}_\sigma$ model to ensure identical temperature variations of basic properties, such as $\Phi(T)$, $L(T)$, and $C_V(T)$, in these two models when they are characterized by a common enthalpy $\Delta h_p$ and a common entropy $\Delta s_p$ of propagation. More specifically, the existence of the correspondence between these model implies that the magnitude of the cooperativity parameter $m$ is directly related to the entropy difference $\Delta s_a - \Delta s_p$ in the $\mathcal{A}_\sigma$ model.

Further examination of the $\mathcal{FA}m$, $\mathcal{A}_\sigma$, $\mathcal{FA}$, and $\mathcal{A}$ models leads to the introduction of thermodynamic measures for the extent of cooperativity ($m_{\text{eff}}$), the degree of transition rounding ($\delta_h$), and the breadth of the self-assembly transition ($D$) that can be generally applied to essentially *all* equilibrium self-assembling systems. Within this generalization, the cooperativity parameter $m_{\text{eff}}$ quantifies the extent to which the self-assembly process resembles a true thermodynamic phase transition. A separate measure of transition rounding $\delta_h \equiv \Delta h_{\text{vH}}/\Delta h_p$ coincides with the often reported thermodynamic cooperativity parameter $\kappa_h \equiv \Delta h_{\text{vH}}/\Delta h_{\text{cal}}$, but we find that these ratios alone are generally not true measures of cooperativity. Our calculations demonstrate, for instance, that values of $\kappa_h$ for the uncooperative $\mathcal{FA}$ model and a cooperative $\mathcal{A}_\sigma$ model ($\sigma \approx 2$) are very similar. An obvious advantage of using the parameter $\delta_h$ instead of $\kappa_h$ is that the former, but not the latter, always approaches unity when self-assembly transition is very sharp. Both parameters $\delta_h$ and $\kappa_h$ can be determined from experimental data for the polymerization (self-assembly) transition lines $T_p = T_p(\phi_1^0)$. The third parameter $D$ introduced by us is particularly useful for quantifying the broadness of the transition when the data for the order paramater $\Phi(T)$ are available. Small $D$ corresponds to a sharp transition, while large $D$ indicates a broad transition. It is often difficult to deduce *a priori* the presence and nature of the interactions that lead to cooperative self-assembly. Given this situation, we summarize some experimentally observable signatures of cooperativity that we have previously found in our theoretical studies[19,74,59] of equilibrium polymerization. These thermodynamic signatures are in accordance with features of cooperative self-assembly that are identified in the biological literature,[18] and our analysis provides insight into this phenomenology.

Although we explain how the constraints of thermal and chemical activation processes can regulate cooperativity in the formation of equilibrium polymers, our analysis does not cover all possible mechanisms of cooperative assembly. For instance, evidence exists that other nonlocal constraints on the assembly process can likewise influence transition cooperativity. Specifically, the introduction of possible ring formation[100] as a constraint on the self-assembly process of the $\mathcal{FA}$ system causes the average cluster mass to increase in an approximately linear fashion, which is one signature of cooperative assembly described above. The presence of inhibitory molecules that terminate rather than initiate polymerization growth can likewise be expected to modulate transition cooperativity (although systematic theoretical treatment is unavailable). For example, recent work demonstrates[26] that the addition of "chain stoppers" or inhibitor additives limits the size of growing chains in solution in a similar fashion to the behavior produced by the addition of a chemical activator or initiator additives.[19,42] Undoubt-

edly, cooperativity can be tuned through the addition of either initiator or "inhibitor" species that act like molecular chaperones for the self-assembly process.

Multifunctional associations provide another basic mechanism for cooperativity in self-assembly that has received limited attention. The presence of multifunctional interactions among self-assemblying particles facilitates the emergence of elastic interactions that are defined in terms of collective coordinates describing the geometry of the newly organizing structure. Specifically, these interactions may be due to surface tension, as emphasized in modeling of micelle formation[101] and domain structures in lipid chloresterol mixtures,[102] or due to surface area dilatational elastic interactions that emerge in the formation of protein cages[43] and vesicles.[103] [The incorporation of these interactions in the $\mathcal{FA}$ model (or the $\mathcal{FA}m$ model[102]) leads to the appearance of organized structures at low temperatures where $m$ is regulated by elastic interactions.] Clearly, multifunctional interactions and collective interactions in particle assembly systems influence the cooperativity of self-assembly.

The formation of multifunctional associations often requires the production of activated or "nucleated" species to initiate the ordering process (polymerization). In such systems, the self-assembled structures are either disordered or ordered network structures, fibers, or sheetlike structures, as computationally found by Van Workum and Douglas,[91] who demonstrated a dramatic alteration in the character of the self-assembly process with a change in the functionality of association. Particles with a predominantly dipolar potential interaction self-assemble into chains that closely follow the noncooperative $\mathcal{FA}$ model,[21] while switching to potentials with a discrete rotational symmetry and multifunctionality (e.g., square quadrupole potential) leads to self-assembly with the hallmarks of a highly cooperative assembly process.[18] A large body of experimental evidence indicates that the self-assembly of even "random" network structures (thermally reversible gels) from particles or polymers exhibiting unsymmetric multifunctional interactions tends to be relatively sharp, with well-defined critical gelation concentrations,[18,19] which again is suggestive of transition cooperativity. Unfortunately, the factors controlling this cooperativity are largely unknown at present. Certainly, the common statement that cooperative self-assembly *must* involve multifunctional interactions[18] is incorrect given our results, but it may well be prevalent in systems having multifunctional interactions, as many biologists have suggested.

Finally, molecular self-assembly in cells and biological media often occurs under conditions of geometrical confinement, either by particle localization into cavities similar in dimensions to the organizing structures or confinement due to surrounding molecules that "crowd" the organizing molecules or particles.[104] Apart from the role of these confining interactions in stabilizing or destabilizing the assembly process (shifting the self-assembly temperature), the nonlocal confinement constraints can alter the cooperativity of the self-assembly process as observed in the self-assembly of sulfur into polymer chains under confinement conditions.[105] Because of its biological relevance, the study of variations in cooperativity induced by confinement interactions represents another attractive field for future investigation.

## ACKNOWLEDGMENTS

This work is supported, in part, by the Joint Theory Institute which is funded by Argonne National Laboratory and the University of Chicago and by NSF Grant No. CHE-0749788. We thank Ka Yee Lee and Peter Zapol for helpful discussions.

[1] P. J. W. Debye, Ann. N.Y. Acad. Sci. **51**, 575 (1949).
[2] H. Wennerström and B. Lindman, Phys. Rep. **52**, 1 (1979).
[3] M. T. A. Evans, M. Phillips, and M. N. Jones, Biopolymers **18**, 1123 (1979).
[4] T. Liu, Z. Ahou, C. Wu, B. Chu, D. K. Schneider, and V. M. Nace, J. Phys. Chem. B **101**, 8808 (1997); T. Liu, Z. Zhou, C. Wu, V. M. Nace, and B. Chu, *ibid.* **102**, 2875 (1998).
[5] Y. Kukmine, K. Inomata, and T. Nose, Polymer **41**, 5367 (2000).
[6] L. A. Marky and K. J. Breslauer, Biopolymers **26**, 1601 (1987).
[7] L. A. Murky, N. R. Kallenbach, K. A. McDonough, N. C. Seeman, and K. J. Breslauer, Biopolymers **26**, 1621 (1987).
[8] W. K. Kegel, J. Phys. Chem. A **108**, 1919 (2004).
[9] P. Ceres and A. Zlotnick, Biochemistry **41**, 11525 (2002).
[10] A. Zlotnick, Virology **315**, 269 (2003).
[11] W. K. Kegel and P. van der Schoot, Biophys. J. **86**, 3905 (2004).
[12] A. F. Riggs, J. Exp. Biol. **201**, 1073 (1998).
[13] W. E. Royer, Jr., H. Zhu, T. A. Gorr, J. F. Flores, and J. E. Knapp, J. Biol. Chem. **208**, 27477 (2005).
[14] Y. Nam, P. Sliz, W. S. Pear, J. C. Aster, and S. C. Blacklow, Proc. Natl. Acad. Sci. U.S.A. **104**, 2103 (2007).
[15] D. Iber, J. Clarkson, M. D. Yudkin, and I. D. Campbell, Nature (London) **441**, 371 (2006).
[16] M. Ptashne, Philos. Trans. R. Soc. London, Ser. A **361**, 1223 (2003).
[17] M. E. Cates and S. J. Candau, J. Phys.: Condens. Matter **2**, 6892 (1990).
[18] L. Romberg, M. Simon, and H. P. Erickson, J. Biol. Chem. **276**, 11743 (2003); M. R. Caplan and H. P. Erickson, *ibid.* **278**, 13784 (2003).
[19] J. Dudowicz, K. F. Freed, and J. F. Douglas, J. Chem. Phys. **119**, 12645 (2003).
[20] F. Sciortino, E. Bianchi, J. F. Douglas, and P. Tartaglia, J. Chem. Phys. **126**, 194903 (2007).
[21] K. Van Workum and J. F. Douglas, Phys. Rev. E **71**, 031502 (2005).
[22] S. Huecas and J. M. Andreu, J. Biol. Chem. **278**, 46146 (2003).
[23] E. Bibb and J. Lutkenhaus, Nature (London) **354**, 161 (1991).
[24] E. T. Adam and M. S. Lewis, Biochemistry **7**, 1044 (1968).
[25] W. Donnhauser, J. Chem. Phys. **48**, 1911 (1968); W. Donnhauser and L. W. Bahe, *ibid.* **40**, 3058 (1964).
[26] R. P. Sijbesma, F. H. Beijer, L. Brunsveld, B. J. B. Folmer, J. H. K. Hirschberg, R. F. M. Lange, J. K. L. Lowe, and E. W. Meijer, Science **278**, 1601 (1997).
[27] X. Murthy and X. Tyagi, J. Chem. Phys. **117**, 3837 (2002).
[28] W. Dannhauser and L. W. Bahe, J. Chem. Phys. **40**, 3058 (1964).
[29] P. Terech, V. Schaffhauser, P. Maldivi, and J. M. Guenet, Langmuir **8**, 2104 (1992).
[30] P. Terech, Ber. Bunsenges. Phys. Chem. **102**, 1630 (1992).
[31] P. Terech and R. G. Weiss, Chem. Rev. (Washington, D.C.) **97**, 3133 (1997).
[32] K. Rah, K. F. Freed, J. Dudowicz, and J. F. Douglas, J. Chem. Phys. **124**, 144906 (2006).
[33] G. Kegeles, Indian J. Biochem. Biophys. **29**, 97 (1991).
[34] G. Kegeles, J. Phys. Chem. **83**, 1728 (1979).
[35] C. H. C. Huang, M. S. Tai, and G. Kegeles, Biophys. Chem. **20**, 89 (1984).
[36] C. G. de Kruif and V. Ya Grinberg, Colloids Surf., A **210**, 183 (2002).
[37] L. M. Mikheeva, N. Grinberg, V. Ya Grinberg, A. R. Khokhlov, and C. G. de Kruif, Langmuir **19**, 2913 (2003).
[38] J. E. O'Connell, V. Ya Grinberg, and C. G. de Kruif, J. Colloid Interface Sci. **258**, 33 (2003).
[39] I. Portnaya, U. Cogan, Y. D. Livney, O. Ramon, K. Shimoni, M. Rosenberg, and D. Danino, J. Agric. Food Chem. **54**, 5555 (2006).
[40] R. Pool and P. G. Bolhius, Phys. Rev. Lett. **97**, 018302 (2006).
[41] F. Oosawa and M. Kansai, J. Mol. Biol. **4**, 10 (1962).

[42] J. Dudowicz, K. Freed, and J. F. Douglas, J. Chem. Phys. **111**, 7116 (1999).
[43] R. Nossal, Macromol. Symp. **227**, 17 (2005); R. Nossal, Traffic (Oxford, U. K.) **2**, 138 (2001); A. J. Jin and R. Nossal, Biophys. J. **65**, 1523 (1993); J. Li, M. Dao, C. T. Lim, and S. Suresh, *ibid.* **88**, 3707 (2005); V. I. Uricanu, M. H. G. Duits, and J. Mellema, Langmuir **20**, 5079 (2004).
[44] M. N. Artyomov and K. F. Freed, J. Chem. Phys. **123**, 194906 (2005).
[45] V. Tobolsky and A. Eisenberg, J. Am. Chem. Soc. **81**, 780 (1959).
[46] V. Tobolsky and A. Eisenberg, J. Colloid Sci. **17**, 49 (1962).
[47] M. L. Mansfield, Phys. Rev. E **66**, 016101 (2002).
[48] G. ten Brinke and F. E. Karasz, J. Chem. Phys. **79**, 2065 (1983).
[49] P. M. Pfeuty and J. C. Wheeler, Phys. Rev. A **27**, 2178 (1983).
[50] J. Dudowicz, K. F. Freed, and J. F. Douglas, J. Chem. Phys. **112**, 1002 (2000).
[51] J. Dudowicz, K. F. Freed, and J. F. Douglas, Phys. Rev. Lett. **92**, 045502 (2004).
[52] Formally, the expression in Eq. (41) can be obtained by taking the limit $m \to 1$ in Eq. (31).
[53] F. W. Starr and F. Sciortino, J. Phys.: Condens. Matter **18**, L347 (2006).
[54] See Sec. IV F of Ref. 65.
[55] N. A. Anderson, L. J. Richter, J. C. Stephenson, and K. A. Briggman, J. Am. Chem. Soc. **129**, 2094 (2007).
[56] D. Levy and K. A. Briggman, Langmuir **23**, 7155 (2007).
[57] W. H. Kirchoff and I. W. Levin, J. Res. Natl. Bur. Stand. **92**, 113 (1987).
[58] S. C. Greer, J. Phys. Chem. B **102**, 5413 (1998).
[59] J. F. Douglas, J. Dudowicz, and K. F. Freed, J. Chem. Phys. **127**, 224901 (2007).
[60] J. Stambaugh, K. Van Workum, J. F. Douglas, and W. Losert, Phys. Rev. E **72**, 031301 (2005).
[61] J. C. Wheeler, S. J. Kennedy, and P. Pfeuty, Phys. Rev. Lett. **45**, 1748 (1980); J. C. Wheeler and P. Pfeuty, Phys. Rev. A **24**, 1050 (1981); S. J. Kennedy and J. C. Wheeler, J. Chem. Phys. **78**, 953 (1983); S. J. Kennedy and J. C. Wheeler, *ibid.* **78**, 1523 (1983); J. C. Wheeler and P. Pfeuty, Phys. Rev. Lett. **46**, 1409 (1981); J. C. Wheeler, *ibid.* **53**, 174 (1984); J. Chem. Phys. **81**, 3635 (1984).
[62] Activated polymerization becomes a first order transition rather than a second order transition in one spatial dimension in the limit of high cooperativity [see P. M. Pfeuty and J. C. Wheeler, Phys. Rev. A 27, 2178 (1983)].
[63] J. Lipfert, J. Franklin, F. Wu, and S. Doniach, J. Mol. Biol. **349**, 648 (2005).
[64] The effective entropy of assembly is also renormalized to a similar degree by transition rounding.
[65] J. F. Douglas, J. Dudowicz, and K. F. Freed, J. Chem. Phys. **125**, 144907 (2007).
[66] W. Burchard, Makromol. Chem., Macromol. Symp. **18**, 1 (1988); **39**, 179 (1990).
[67] V. Degiorgio, R. Piazza, M. Corti, and C. Minero, J. Chem. Phys. **82**, 1025 (1985).
[68] M. Corti, C. Minero, and V. Degiorgio, J. Phys. Chem. **88**, 309 (1984).
[69] A. P. Minton, Methods Enzymol. **295**, 127 (1998).
[70] M. Jimenez, G. Rivas, and A. P. Minton, Biochemistry **46**, 8373 (2007).
[71] G. J. Howlett, A. P. Minton, and G. Rivas, Curr. Opin. Chem. Biol. **10**, 430 (2006).
[72] A. K. Attri and A. P. Minton, Anal. Biochem. **337**, 103 (2005).
[73] D. G. Leist and L. Hui, J. Phys. Chem. **93**, 7547 (1989).
[74] J. Dudowicz, K. F. Freed, and J. F. Douglas, J. Chem. Phys. **113**, 434 (2000).
[75] A. Milchev, Polymer **34**, 362 (1993); Y. Rouault and A. Milchev, Phys. Rev. E **51**, 5905 (1995); A. Milchev and D. P. Landau, *ibid.* **52**, 6431 (1995); J. Chem. Phys. **104**, 9161 (1996); J. P. Wittmer, A. Milchev, and M. E. Cates, Europhys. Lett. **41**, 291 (1998).
[76] H. J. A. Zweistra and N. A. M. Besseling, Phys. Rev. E **96**, 078301 (2006).
[77] P. Mukerjee, J. Phys. Chem. **76**, 565 (1972).
[78] P. Schurtenberger and C. Caraco, J. Phys. II **3**, 1279 (1993); **4**, 305 (1994); P. Schurtenberger, C. Caraco, F. Tiberg, and O. Regev, Langmuir **12**, 2894 (1996).
[79] G. J. M. Koper, C. Cavaco, and P. Schurtenberger in *25 Years of Non-Equilibrium Thermodynamics*, edited by J. J. Brey, J. Marro, J. M. Rubi, and M. San Miguel (Springer-Verlag, Berlin, 1995), p. 363.
[80] A. Stradner, H. Sedgwick, F. Cardinaux, W. C. K. Poon, S. U. Egelhaaf, and P. Schurtenberger, Nature (London) **432**, 492 (2004).
[81] A. J. Rahedi, J. F. Douglas, and F. W. Starr, J. Chem. Phys. **128**, 024902 (2008).
[82] G. Orkoulas, S. K. Kumar, and A. Z. Panagiotopoulos, Phys. Rev. Lett. **90**, 048303 (2003).
[83] F. Afroze, E. Nies, and H. Berghmans, J. Mol. Struct. **554**, 55 (2001).
[84] G. Malescio, G. Franzese, G. Pellicane, A. Skibinsky, S. V. Buldyrev, and H. E. Stanley, J. Phys.: Condens. Matter **14**, 2193 (2002).
[85] Y. Katayama, T. Mizutani, W. Utsumi, O. Shimomura, M. Yamakata, and K. Funakoshi, Nature (London) **403**, 170 (2000).
[86] F. W. Starr and F. Sciortino (submitted to Proc. Nat. Acad. Sci).
[87] T. M. Rascshke, J. Tsai, and M. Levitt, Proc. Natl. Acad. Sci. U.S.A. **98**, 5965 (2001); R. H. Wood and P. T. Thompson, *ibid.* **87**, 946 (1990).
[88] J. J. Kozak, W. S. Kinight, and W. Kauzmann, J. Chem. Phys. **48**, 675 (1968).
[89] S. Shimizu and H. S. Chan, J. Chem. Phys. **115**, 1414 (2001); **115**, 3424 (2001).
[90] P. G. de Gennes, C. R. Acad. Sci., Ser. II: Mec., Phys., Chim., Sci. Terre Univers **313**, 1117 (1991); Pure Appl. Chem. **64**, 1585 (1992).
[91] K. Van Workum and J. F. Douglas, Phys. Rev. E **73**, 031502 (2006).
[92] W. Kauzmann, Biophys. J. **4**, 43 (1963).
[93] D. A. Brant and P. J. Flory, J. Am. Chem. Soc. **87**, 663 (1965).
[94] H. Kaya and H. S. Chan, Proteins **52**, 510 (2003); Phys. Rev. Lett. **85**, 4823 (2000); Proteins **40**, 637 (2000).
[95] A. Kolinski, D. Gront, P. Pokarowski, J. Skolnick, and D. Danforth, Biopolymers **69**, 399 (2003).
[96] T. R. Weikl, M. Palassini, and K. A. Dill, Protein Sci. **13**, 822 (2004).
[97] M. A. A. Barbosa, L. G. Garcia, and A. F. Pereira de Araujo, Phys. Rev. E **72**, 051903 (2005).
[98] C. Dalle-Ferrier, C. Thibierge, C. Alba-Simionesco, L. Berthier, G. Biroli, J.-P. Bouchaud, F. Ladieu, D. L'Hote, and G. Tarjus, Phys. Rev. E **76**, 041510 (2007).
[99] Self-assembly also underlies glass formation (see Ref. 65), which implies that the metrics developed for quantifying cooperativity in self-assembling systems also have relevance for the description of glass formation.
[100] L. S. Pam, L. L. Spell, and J. T. Kindt, J. Chem. Phys. **126**, 134906 (2007).
[101] J. N. Israelachvili, *Intermolecular Surface Forces* (Academic, London, 1992).
[102] Y. Hu, K. Meleson, and J. N. Israelachvili, Biophys. J. **91**, 444 (2006).
[103] H. T. Jung, B. Coldren, J. A. Zasadzinski, D. J. Iampietro, and E. W. Kaler, Proc. Natl. Acad. Sci. U.S.A. **98**, 1353 (2001).
[104] A. P. Minton, J. Pharm. Sci. **94**, 1668 (2005); J. Biol. Chem. **276**, 10577 (2001); M. Hayer-Hartl and A. P. Minton, Biochemistry **45**, 13356 (2006); A. P. Minton, Biophys. J. **63**, 1090 (1992); F. Takagi, N. Koga, and S. Takodo, Proc. Natl. Acad. Sci. U.S.A. **100**, 11367 (2003).
[105] A. G. Kalampounias, K. S. Andrikopoulos, and S. N. Yannopoulos, J. Chem. Phys. **119**, 7543 (2003).